Effectiveness of Polyurethane Foam Coated Chitosan/MXene Nanoparticles as Low-Cost Adsorbent for Heavy Metal Removal

By

Amir Younas

Registration No. 00000277756

A thesis submitted in partial fulfillment of the requirements for the degree of

Master of Science

in

Environmental Engineering

Institute of Environmental Sciences and Engineering
School of Civil and Environmental Engineering
National University of Sciences and Technology
Islamabad, Pakistan
2022

APPROVAL CERTIFICATE

Certified that the contents and form of the thesis entitled

"Effectiveness of Polyurethane foam coated Chitosan/MXene nanoparticles as low-cost adsorbent for heavy metal removal"

Submitted by

Mr. Amir Younas

Has been found satisfactory for partial fulfillment of the requirements of the degree of Master of Science in Environmental Engineering.

Supervisor: .....
Dr. Waqas Qamar Zaman
Assistant Professor
IESE, SCEE, NUST

Co-Supervisor: .....
Dr. Waheed Miran
Assistant Professor
SCME, NUST

GEC Member: …….
Dr. Muhammad Ali Inam
Assistant Professor
IESE, SCEE, NUST

GEC Member: ……..
Dr. Zaeem Bin Babar
Assistant Professor

ACCEPTANCE CERTIFICATE

It is certified that final copy of MS/MPhil Thesis entitled **"Effectiveness of Polyurethane foam coated Chitosan/MXene nanoparticles as low-cost adsorbent for heavy metal removal"** written by Mr. Amir Younas (Registration No: 00000277756) of IESE (SCEE) has been vetted by the undersigned, found complete in all respects as per NUST Statues/Regulations, is free of plagiarism, errors, and mistakes, and is accepted as partial fulfillment for the award of MS/MPhil degree. It is further certified that necessary amendments as pointed out by GEC members of the scholar have also been incorporated in the said thesis.

Supervisor: ……

Dr. Waqas Qamar Zaman

Dated: …….

Head of Department: ……

Dated: ……

Dean/Principal: …….

Dated: ……..

DECLARATION CERTIFICATE

I declare that this research work titled **"Effectiveness of Polyurethane foam coated Chitosan/MXene nanoparticles as low-cost adsorbent for heavy metal removal"** is my own work. The work has not been presented elsewhere for assessment. The material that has been used from other sources as been properly acknowledged/referred.

Student Signature: ……...

Student Name: Amir Younas

Registration No. 00000277756

PLAGIARISM CERTIFICATE

I certify that this research work titled "Effectiveness of Polyurethane foam coated Chitosan/MXene nanoparticles as low-cost adsorbent for heavy metal removal" is my own work. Thesis has significant new work as compared to already published or under consideration to be published elsewhere. The thesis has been checked using TURNITIN and found within limits as per HEC plagiarism Policy and instructions issued from time to time.

Amir Younas

Registration No. 00000277756

…..……..……..

Signature of Supervisor

Date: ……

DEDICATION

"Dedicated to my exceptional parents, adored siblings,

and my friends whose tremendous support and

cooperation led me to this wonderful accomplishment".

ACKNOWLEDGEMENTS

First and foremost, I acknowledge that it is by the grace of Allah Almighty that I have been able to complete this manuscript. With respect to the Holy Prophet (P.B.U.H) whose life is the model I am trying to base my life around.

Next, I express my utmost thanks to my supervisor Dr. Waqas Qamar Zaman, who has supported and guided me throughout my research. His keen interest and valuable suggestions have helped me overcome all obstacles encountered during my research work. I will forever be thankful for his incredible guidance, encouragement, and sympathetic attitude during the entire period of my research.

I would like to pay my gratitude to Dr. Waheed Miran, Dr. Muhammad Ali Inam and Dr. Zaeem Bin Babar, for their support and meaningful guidance. I thank Dr. Muhammad Taqi Mehran and Mr. Anees Khan for their continuous assistance and support during my research.

This acknowledgement would be inadequate whitout my sincere and heartedly thanks to my loving parents for their sacrifices, prayers, and affections without that it would have been nearly impossible to achieve my goals. My sincerest thanks to all my friends at IESE for their support and help during my MS course at NUST. I would also thank other institutes for their continuous support and encouragement throughout my time at NUST. Last but not the least I would like to thank all the laboratory staff at IESE for their help and cooperation.

Amir Younas

TABLE OF CONTENTS

ACRONYMS AND ABBREVIATION

CH	Chitosan
CPU	Chitosan @ PUF
Cr (III)	Trivalent Chromium
Cr (VI)	Hexavalent Chromium
IARC	International Agency for Research on Cancer
MC1@PUF	1 layer MX@CH@PUF
MC2@PUF	3 layer by layer MX@CH@PUF
MCPU	MXene@Chitosan@PU Foam
MPU	MXene@PUF
MX	MXene
MX@PU	MXene@PU Foam
PFO	Pseudo First Order
PPU	Pristine Polyurethane Foam
PSO	Pseudo Second Order
PUF	Polyurethane Foam
WHO	World Health Organization

LIST OF TABLES

LIST OF FIGURES

Abstract

Heavy metal removal from wastewater remains a paramount challenge with rapid industrialization and its ubiquitous utilities. Currently, the generation of clean water and environmental protection are two indispensable/requisite areas for a sustainable society. Two-dimensional (2D) materials' applicability in water treatment is continuously accelerating by enabling new discoveries. Recently, MXenes generated tremendous popularity in the 2D materials family due to unique physicochemical properties and stability that as adsorbents make them attractive for the removal of heavy metals. Although the adsorption performance of MXenes may compete effectively with other nanomaterials adsorbents, the interplay with different materials is insufficient/inadequate/restricted for further development of low-cost material for commercial applications. Herein, a potential MXene (Ti_3AlC_2) combined with Chitosan, an abundant crustacean's polymer, as surfactant on polyurethane foam (PUF) for the removal of toxic hexavalent chromium from synthetic wastewater via adsorption process. The sorption capabilities of PUF for wastewater were enhanced using MXene nano-sheets adherence to the pores, while Chitosan beforehand was used as a surfactant for constructive deposition of MXene nano-sheets. Positively charged Chromium (VI) ions are adsorbed on negatively charged MXene via electrostatic attraction and ion exchange mechanism. An assay of assessment is done through a series of batch and fixed-bed column studies using PUF cubes coated with Chitosan and three different layers of MXene over Chitosan. Complete removal of hexavalent chromium in 2 hours has been observed in the batch process, which is quite promising. Detailed characterization techniques were employed to identify elements, structural type, and chemical functionality. Additionally, Langmuir and Freundlich kinetic model for batch operation confirms the chemisorption during the process. Furthermore, briefed fixed bed column experiments were performed to check the continuous operation stability of the adsorbent for future perspective. The experimental study attributed the favorable and economically sustainable aspect of potential adsorbent in water treatment applications as compared to the usage in an individual capacity in powder form.

CHAPTER 1

INTRODUCTION

1.1 Background

As economic output continues to expand globally, consumption of water and natural resources grows relentlessly. The effects are visible as water over-abstraction, water and land degradation, climate change and emerging extinction crises. These are creating interrelated risks for economics, people and ecosystems that are unprecedented in human history. Water is indispensable for human health, food security and biodiversity, and for industrial growth, energy supply and urban development. Global demand for freshwater has grown multifold in recent years, a trend that cannot be sustained. Water is essentially a key parameter to the transformative ambition of the 2030 Agenda. (*Innovative Water Solutions for Sustainable Development SUMMARY*, 2014; WHO, 2017) Water treatment often suffers from a dilemma between economy and efficient applicability. Therefore, Water solutions are needed at all levels as water pollution holds back development, aggravates inequality and poverty, and exacerbate food scarcity, vulnerability, conflict, and fragility.

Many countries are facing serious environmental problems of chromium pollution in waters and groundwaters. Rest aside natural, some anthropogenic activities like dye and pigment manufacturers, galvanometry, electroplating, leather and mining cause undesired efflux of Chromium (VI) anions. Among the possible stable forms of chromium, hexavalent chromium is the most toxic, producing liver and kidney damage, internal hemorrhage and respiratory disorders(Gupta & Babu, 2009; Rodrigues et al., 2019; X. S. Wang et al., 2009). It has been indicated as carcinogenic and detrimental to humans by International Agency for Research on Cancer (IARC). Hexavalent Chromium found active in a wide range of genotoxicity tests, once it is introduced into human cells, it can manifest favoring cancer onset, genomic instability and apoptosis(Wise et al., 2022). World Health Organization permissible limit for hexavalent chromium Cr(VI) is 0.05 mg/L (WHO, 2017). Cr (VI) can enter the human body by breathing air, consuming affected food, or drinking chromium containing water. Due to its existence in the environment in several forms, the removal of toxic Cr(VI) has gained extensive attention (Liang et al., 2020).

Various methods utilized for heavy metal removal from wastewater include precipitation, membrane filtration, electrocougulation, ion exchange and adsorption. However, most of the technologies have technical and economical limitations, for instance, inadequate removal of metals, production of sludge and high energy requirements which impede their widescale development and commercialization. Physico-chemical methods exihibits high performances in removing hexavalent chromium, but most of them has high costs of the operations (Gorzin & Bahri Rasht Abadi, 2018; Patel, 2019). For practical application, adsorption method seems to be most feasible wastewater treatment technology owing to its environmental and economical sustainability (Niu et al., 2021). The adsorption process necessitates a low cost and highly efficient adsorbent with high removal proficiency and high adsorption capability under various conditions (Danish et al., 2013).

For effective adsorption of Cr (VI) from an aqueous phase, the prospective adsorbent must have a large surface area and negatively charged functional groups. MXenes are a recent category of two-dimensional materials that have interesting properties and are utilised in a wide range of fields. MXenes are a good option for ion-adsorption owing to their large specific surface area, hydrophilic nature, abundant surface functional groups, ion exchange capability, chemical stability, and environmentally friendly nature (Yang et al., 2021). MXenes are formed from MAX phase ($M_{n+1}AX_n$, Here "M" represents a transition metal, "A" corresponds to III-A or IV-A group elements, and X is C or N) by etching away A layer (Shahzad et al., 2017; Yaqub et al., 2021).

Herein, we report the adsorption of Cr (VI) by using Chitosan and MXene nanoparticles in a low-cost yet effective way by utilizing polyurethane foam in a batch and continuous fixed-bed process. Fixed bed studies were opted to minimize the wastage of nanoparticles using PU foam selectivity and check its stability in continuous operation. The affinity of polyurethane foam with the nanoparticles increased the removal efficiency of Cr (VI) which is an indicator of its commercial viability.

1.2 Problem Statement

Growing industrialization and urbanization have posed a significant threat to the quality of groundwater. A potential environmental and public health concern for millions of people worldwide is groundwater contamination with chromium metal from the tanning and leather industry. In natural environment, chromium occurs as Chromium (III) and Chromium (VI), while Chromium (VI) is more solvable and perilous than Cr (III). Cr (VI) can cause stern health issues like lungs damage, skin irritation and even cancer.

On the other hand, Chitosan as an abundant biopolymer is cheap and effective in heavy metal removal. MXene with many applications has a lot of potential in water treatment which makes it a multidisciplinary material in the market. Cost is the major concern when talking about water treatment. Many industries are reluctant in developing countries due to the extensive capital involved in water treatment operations. For that reason, low-cost techniques and materials are required to explore for bringing all the stakeholders to indulge in the practices that go along with UN sustainable development goals. Consequently, utilizing low-cost polyurethane foam as a support material for water treatment is a valuable process. Adsorption, as opposed to traditional methods, is a sustainable and profitable method for the management of toxic elements such as chromium.

1.3 Research Objectives

The research objectives of this research work are;

- Synthesis and characterization of Chitosan/MXene nanoparticles coated PU foam adsorbents.
- Comparison of non-functionalized and functionalized adsorbents in batch and continuous process for removal of Hexavalent Chromium from wastewater.

CHAPTER 2

LITERATURE REVIEW

2.1 Background:

One of the major concerns facing the world today is environmental pollution. Many countries along with Pakistan are facing this problem due to ever-growing population rate, consumption of natural and synthetic resources, industrialization, and heavy dependency on fossil fuels. Every aspect of our life contributes to air pollution, water contamination or soil pollution one way or the other. Rapid industrialization is a major contributor to water pollution.

Water is considered as an essential commodity for sustaining life and environment that is always thought to be an inexhaustible resource. In this new era, over eight billion humans, is facing a serious water crisis. Pakistan is a water stressed country, with per capita water accessibility of only 930 m^3 annually. Rapid industrialization and urban development, along with increasing irrigation needs for agriculture, are depleting both the quantity and quality of the country's water resources, have negative impact on the agricultural output and the health of the population (Reale, 2021). The effluent released, contaminates freshwater bodies like rivers, lakes, and fresh underground water reservoirs. This renders the water unsuitable for domestic usage.

Toxic metals in the environment are a worldwide concern due to their negative impacts on humans and aquatic flora and fauna. Heavy metal dumping to the soils and water causes substantial environmental risks due to its non-decomposable nature (Briffa et al., 2020). Arsenic (Agrafioti et al., 2014; Fard et al., 2021), Lead (Dong et al., 2019a), and Chromium (H. Wang et al., 2020) are among the most toxic heavy metals. Researchers around the world are concentrating on removinf or reducing the concentration of these heavy metals from wastewater up to acceptable limits.

2.2 Introduction of Chromium:

Chromium is a heavy metal that displays several properties depending on its valence states, chromium (III), a trace element, is crucial for human body in contrast hexavalent chromium (VI) is lethal and oxidative (Monga et al., 2022). Chromium and its compounds are mainly utilized in, metallurgy, and pigments. Effluents from these

industries are disposed into rivers, ponds, and oceans and directly effecting living organisms due to its carcinogenic and mutagenic nature. Exposure of heavy metals like chromium even in small concentrations is hazardous and its removal is still a challenging task for modern researchers.

Chromium compounds are only noticed in trace amounts in water; however, the element and its compounds can be disposed into surface water by a variety of industries. Chromium is present in both natural and man-made sources. Geological ultramafic and basaltic rocks, especially serpentinites, are natural sources; these rocks are frequently replaced by amphiboles, garnets, micas, pyroxenes, and spinel. Man-made sources include tanneries, metal finishing, cooling towers, pigment synthesis, dyeing, and chemical industries that use high chromium salts (Aregahegn, 2021; Velusamy et al., 2021).

Chromium oxide (Cr_2O_3) has become a widespread material for research purposes due to its superb physicochemical properties. Chromium is used to tint glass emerald, green. Chromium compounds are used as mordents in the textile industry, as well as anodizing aluminum in the aerospace and other industries. Because of its high melting point, medium thermal expansion, and crystalline structure stability, chromite has been used in the refractory industry to form bricks and shapes. Chromium is employed in alloy fabrication, alloy steel preparation to improve corrosion and heat resistance, nonferrous alloy manufacturing to impart special qualities to the alloys, insoluble salt production and processing, and moth proofing wool (Hansen et al., 2022). According to the arrangement of the glass and the melting condition, Cr^{3+} and Cr^{6+} ions can coexist in silicate and borate glasses in varying ratios (Zhu et al., 2016). The main function of Chromium in the body is to regulate blood flow, moderate cholesterol levels, contribute to lean muscle mass, promote arterial health, boost the immune system, and stimulate protein synthesis (Alagawany et al., 2021).

2.3 Effects of Chromium:

Cr (III) is required by plants, whereas Cr (VI) is toxic to both plants and animals at low concentrations. Because Cr (III) oxides are only marginally soluble in water, their concentration in water sources is constrained. Under aerobic conditions, hexavalent chromium compounds are stable, but under anaerobic conditions, they have reduced to Cr (III) compounds. In an oxidizing environment, the reverse process is also

a possibility. Chromium concentrations in soils ranging from 500 to 6000 mg/L are not harmful to plants (Chen et al., 2022). Chromium toxicity has a pH-dependent mechanism. Chromium availability to plants is reduced as soluble chromates are converted to insoluble Cr (III) salts. This mechanism safeguards the food chain against excessive chromium levels (Srivastava et al., 2021). Cr (VI) is a poison that is easily absorbed and can be swallowed or inhaled. Skin contact with Cr (VI) can cause vulnerable and genetic defects, as well as cancer, by raiding the respiratory track (Mohamed et al., n.d.). High chromium concentrations due to the disposal of metal products in surface water can affect the gills of fish swimming near to the disposal site (Kahlon et al., 2018).

2.4 Techniques for Chromium Removal

Technologies for Cr (VI) removal include:

- Precipitation
- Membrane technology
- Electrocoagulation
- Ion exchange
- Adsorption

2.4.1 Precipitation

All methods of water and wastewater treatment for metal removal have their advantages and disadvantages. Traditionally, the Chemical – precipitation method is simple but cost-ineffective even at a low concentration of metal ions and produces a large amount of sludge that cannot be easily treated (Ramakrishnaiah & Prathima, 2012). In this process, chemical agents are used to translate heavy metal ions into insoluble precipitates, which are later separated by the filtration process, as shown in Figure 1. Precipitates usually consist of sulfides, phosphates, carbonates, and commonly used hydroxides of alkali and alkali earth metals i.e., NaOH, KOH, $Ca(OH)^2$.

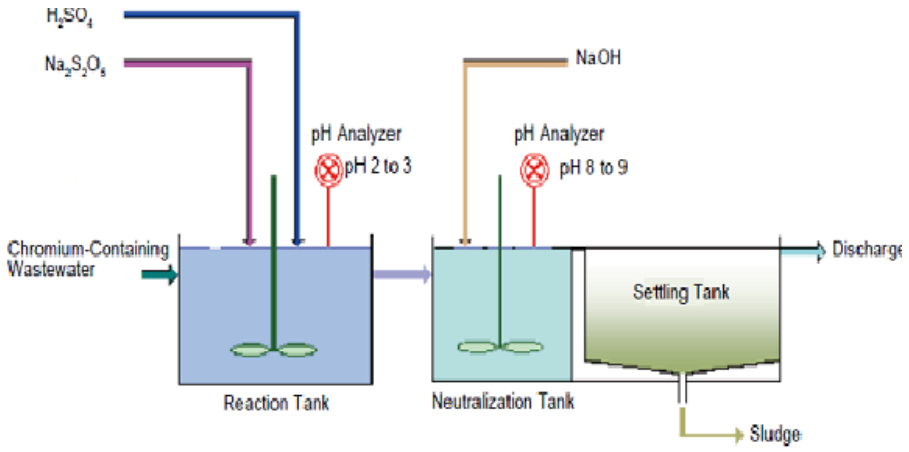

Figure 1: Schematic representation of precipitation process

2.4.2 Membrane Filtration

In the Membrane Filtration method, contaminants are physically separated from water using a porous membrane which only allows water molecules to pass through it while inhibiting the contaminants (Heavy metal ions, Organic molecules, Salt ions, etc.). (Gao et al., 2022; H. Peng & Guo, 2020b)

The main methods of Membrane Filtration are:

(i) Microfiltration (MF) (i) Ultrafiltration (UF) (iii) Nanofiltration (iv) Reverse Osmosis, as shown in Figure 2.

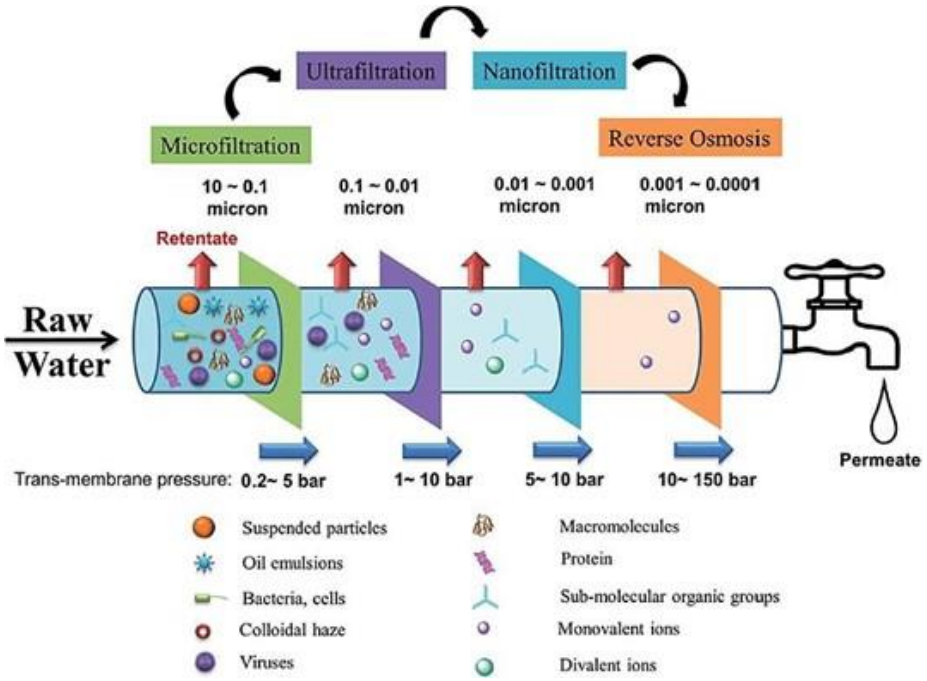

Figure 2: The schematic representation of the membrane process

2.4.2.1 Microfiltration (MF)

In Microfiltration the pore sizes of the membrane are in the range of 0.1 to 10 μm. This process is mainly used in the food and beverage industry to treat wastewater. As Chromium (VI) ions are smaller in size and are difficult to separate by microfiltration or ultrafiltration. Therefore, a chemical modification is considered necessary to mix Cr (VI) ions with the other massive molecules present (Karimi-Maleh et al., 2021). This problem can be solved by modifying the membrane material (Somen et al., 2010). (Doke & Yadav, 2014) used micellar-enhanced microfiltration (MEMF) as a surfactant-based membrane with a cationic surfactant of cetylpyridinium chloride. They discovered that the surfactant-to-chromate ratio was 2.5, which was lower than the CMC best ratio for 99% Cr (VI) removal when using a ceramic titania membrane.

2.4.2.2 Ultrafiltration (UF)

Ultrafiltration has a large similarity to microfiltration but, with membranes having smaller pore sizes ranging from 0.01 to 0.1 μm. sugars, Salts and organic acids are permeable from the membrane while fats, proteins, viruses, polypeptides, and polysaccharides are impermeable. Ultrafiltration (UF) is one of the membrane methods that involves the least amount of pressure. The primary use of UF is to split pollutants with high molecular weight, such as peptides and polysaccharides. Because of their small pore size, UF membranes cannot separate ionic species (Yanhong Zhang et al., 2021).

Kumar Basumatary et al. investigated the exclusion of Cr (VI) in crossflow mode ultrafiltration using MCM-48, MCM-41, and FAU zeolite placed on porous ceramic support UF membranes (Kumar Basumatary et al., 2016). When extreme pressure was used, optimal filtration operation was achieved, whereas denial was high when cross flow rate was low. The removal efficiencies of FAU, MCM-41, and MCM-48 membranes were 82%, 75%, and 77%, respectively. Polymer-enhanced ultrafiltration (PEUF) and micellar-enhanced ultrafiltration (MEUF) membranes are also utilized for the removal of Cr (VI) (Elfeky et al., 2017).

2.4.2.3 Nanofiltration (NF)

Just like Reverse Osmosis, NF membranes consist of a thin film of <1 μm composite layer and a porous layer of 50 to 150μm to selectively remove small ions. Nanofiltration has also been used for the removal of Cr (VI) from wastewater (Wei et

al., 2019). NF300 membrane showed higher removal efficiency as compared to PN400 nanofiltration membrane and removed 97% and 92% Cr (VI) and fluoride ions from dual solution respectively (Gaikwad & Balomajumder, 2017). It was noticed that with an increase in pressure, the refusal of Cr (VI) and fluoride ions also increased, and it will decrease as the feed concentration increased. The removal of Cr (VI) was also accomplished using a thin film-charged surface NF membrane, the surface of which, owing to its negative surface charge, prevents the formation of Cr and other anions (Bohdziewicz, 2000). The results showed an increasing trend as the pH increased. This is due to membrane surface deprotonation, which increased electrostatic repulsion and the production of CrO_4^{2-}.

2.4.2.4 Reverse Osmosis (RO)

Reverse Osmosis uses the tightest membrane which only allows water to pass through it while rejecting all monovalent ions. The reverse membrane (RO) technology is advantageous for the removal of Cr (VI). RO membranes are operated at high pressures to achieve the highest effluent water purity. (Gaikwad & Balomajumder, 2017) used polyamide RO membranes to remove Cr (VI) and fluoride ions from aqueous solution. The results showed that increasing the pressure and decreasing the concentration of Cr (VI) and fluoride ions in the feed increased their removal. When the pH of the solution was raised to 8, removal was also increased. Similar results were obtained for Cr (VI) and fluoride ions using the NF500 membrane.

2.4.3 Electrocoagulation

Electrocoagulation (EC) is an effective method for eliminating impurities from water that involves passing an electric current through metal plates to subvert fine material and counteract the electric charge of impurities, causing them to coagulate (Nidheesh, 2022). A relatively small reactor is required for confined wastewater at low temperature and turbidity. The flocks formed in EC are more stable and resistant to acids when compared to chemical coagulation; however, when aluminum or aluminum sulphates are used in EC, its efficiency for Cr(VI) removal increases 3 times as compared to chemical coagulation (Golder et al., 2007). Two phases involve for the treatment of Cr (VI) includes (H. Peng & Guo, 2020a).

- Reduction to Cr (III)
- Cr (III) parting as hydroxide

2.4.4 Ion Exchange

Ion Exchange is also employed for removing heavy metal ions from contaminated water, it is very effective in the treatment of waste containing low concentrations of heavy metals. Ion exchange resins can exchange ions with other metal ions (Heavy metal ions). The ion exchange is known physicochemical method that implies the replacement of ions between solids and liquids (Hu et al., 2020). and has great success for the removal of Cr (VI). Cr (VI) was removed from water using a variety of ion exchange resins. These resins are composed of a matrix, a three-dimensional molecular network having chemically bonded charged functional groups. Sapari et al. (1996) considered the removal of Cr (VI) from real plating wastewater using synthetic ion exchange resin (Dowex 2-X4) and achieved 100% results. Use of IRN77 and SKN1 cation resins for removal also shows effective results and remove 95% Cr (VI) from water. Adsorption capacities for both IRN77 and SKN1 were 35.38 and 46.34 mg/g respectively (Rengaraj et al., 2001). Some of the important parameters for ion exchange method include resin dose, pH, and initial Cr (VI) concentration (Fu et al., 2013).

The main drawbacks of this process are

- Other competing ions like sulfate, carbonate, and phosphate reduce the removal efficiency.
- The cost of resin, waste disposal and regeneration make the process expensive.
- Treated water contains high levels of chlorides.

2.4.5 Adsorption

Adsorption is one of the most appropriate, competent, and applicable technology for the removal of heavy metals including Cr (VI) (Yujuan Zhang et al., 2018). Researchers have been looking for suitable adsorbents having higher removal efficiencies and higher adsorption capacities for the removal of Cr (VI) from polluted water. For that purpose, variety of adsorbents including natural organic, natural inorganics, and synthetic adsorbents have been considered. These adsorbents have been used in their original form, but their modification i.e., change in chemical structure, cross-linking, and grafting has attracted great attention (Ibrahim et al., 2020). Four mechanisms proposed for the interaction between Cr (VI) and adsorbents are

- Cr (VI) reduction to Cr (III)
- Adsorption through electrostatic forces

- Ion Exchange mechanism
- Complex formation

The adsorption process is greatly enhanced with the discovery of 2D materials like Graphene followed by MXenes. The next chapter will cover a detailed discussion of MXene and its properties as an adsorbent.

2.4.5.1 Characteristics of an Ideal Adsorbent

The particle size of the adsorbents plays a vital role to improve the adsorption efficiency (Hamadi et al., 2001). The important characteristics of an ideal adsorbent are (Bhatnagar & Minocha, 2006).

- It has large surface area
- Adsorbent has uniform pore structure
- It requires less time to reach equilibrium
- It has high chemical and physical strength

2.5 PU foams for Water Treatment:

PU foam is chemically inert and does not possess the risk of health hazards, therefore there is not any exposure limit for PU foam. Owing to their properties like chemical inertness, high surface area, biocompatibility and 3D interconnected skeleton which could attach numerous functional groups for capturing toxic species from water, PU foams share great potential for water remediation. For this purpose, several researchers employed PU foam functionalized with graphene, chitosan and other adsorbents or PU foam composites for the treatment of toxic waste. For example, (Kumari et al., 2016)extracted lignin from a bio waste material (pine needles) and employed it as a polyol in the synthesis of PU foam. Obtained Lignin Polyurethane foam (LPUF) was utilized for the removal of Dyes such as malachite green. LPUF exhibited an adsorption capacity of 80 mgg_{-1} and excellent regeneration performance (collective adsorption of 1.33 gg^{-1} after 20 regeneration cycles) . Hong et al. embedded Carboxymethylated cellulose nanofibrils (CMCNFs) in PU foam and applied it to remove heavy metal ions from industrial wastewater (Hong et al., 2018). CMCNFs are promising bio-sorbent for heavy metal ions. Hong and co-workers successfully removed Cu^{2+}, Cd^{2+}, and Cr^{3+} ions from water with an initial concentration of 50 mg/L. Equilibrium was achieved by soaking PU foam for 72 hours. Prepared PU foam

embedded with CMCNFS exhibited 78.7 mg. g^{-1} Cu^{2+} and 216.1 mg. g^{-1} Cr^{3+} removal with the facile treatment method and achieved excellent recovery and recyclability.

Machado Centenaro et al. studied coated PU foam with chitosan and employed it as a low-cost adsorbent for the Dyes in textile waste (Machado Centenaro et al., 2017). Chitosan-coated PU foam (EPU-Chitosan) exhibited an adsorption capacity of 86.43 mg. g^{-1} towards reactive blue dye RB198. Adsorption was enhanced in an acidic medium because at low pH amino groups of chitosan become protonated and electrostatic interaction between chitosan and sulfonated ions (SO^{3-}) of RB198 dye increases. (Yin et al., 2022) functionalized PU foam with alkoxysilane group to impart hydrophobicity and affinity towards oil and other organics. Salinized PU foam exhibited oil absorption capacity of 75 times of its own weight and maintained 90% absorption after reusing 8 times. The authors also showed continuous oil water separation by filling salinized PU foam in a vacuum cleaner. PU foam is an ideal material for continuous oil-water separation. (M. Peng et al., 2019) prepared a super-hydrophobic polysiloxane coated PU foam for continuous oil water separation and achieved separation up to 300 cycles without losing hydrophobicity. Similarly, (Anju & Renuka, 2020) prepared superhydrophobic/super oleophilic magnetic PU foam by anchoring Fe_3O_4 nanoparticles onto the PU foam skeleton using dopamine self-polymerization, followed by the addition of hydrophobic molecules such as heptadecafluoro-1,1,2,2-tetrahydrodecyltrimethoxysilane (FAS-17) to induce the superhydrophobic transformation. Prepared superhydrophobic PU sponge performed well with stability under corrosive environments, excellent oil-water separation performance under magnetic actuation and in extreme environments (pH=1). (Santos et al., 2017) impregnated lignin in the PU foam skeleton to enhance oil sorption capacity. PU-10 (PU with 10 wt % lignin) exhibited maximum oil sorption capacity of 28.9 g g_{-1} and excellent reusability with 95% absorption capacity after 5 cycles.

2.6 Chitosan

Chitosan, an antimicrobial polysaccharide derived from chitin, is the most abundant polysaccharide after cellulose in the biosphere. Chitosan's biological properties, including biodegradability, non-toxicity, antifungal effects, wound healing enhancement, hemostatic function, and immune system stimulation, make it a favourable material for medical applications. To enhance the impact of chitosan-based

materials, the specific surface area can be increased by creating either nanoscale materials or highly porous architectures.

Table 1: Different Applications of Chitosan (Rinaudo, 2006; Siqueira et al., 2010)

Agriculture	Plant growth can be stimulated by seed coating, frost protection, and time-released fertilizers and nutrients.
Water and waste treatment	Flocculant to clarify water Removal of metal ions Odor reducer
Food and beverages	Fruit can be coated with a protective, fungitoxic, and antibacterial substance to preserve sauces
Cosmetic and toiletries	Creams and lotions maintaining skin moisture Shampoos, hair colorants, hair sprays Oral care (toothpaste, chewing gum)
Biopharmaceutics	Immunology, antitumor agent Hemostatic and anticoagulant Healing, bacteriostasis
Biomedical	Artificial skin Wound dressing Dental implant Bone reconstruction Corneal contact lenses Controlled drug release

Chitosan's structure is shown in Figure 3, which consists of β-(1→4)-linked D-glucosamine units with an undefined quantity of N-acetylglucosamine moieties. The proportion of glucosamine to the sum of glucosamine and N-acetylglucosamine is known as the deacetylation degree (DD), as shown in Equation 1. When the degree of deacetylation is higher than 50%, partially deacetylated chitin can be considered as chitosan (Crini & Badot, 2008).

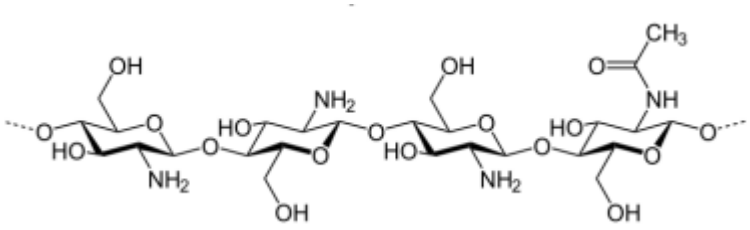

Figure 3: Chemical Structure of Chitosan

$$\text{Degree of Deacetylation} = \frac{\text{Glucosamine}}{\text{Glucoseamine+N-acetylglucosamine}} \quad (1)$$

2.7 MXene

MXene belongs to recently discovered family of 2D transition metal carbides and nitrides. MXenes are prepared by selectively etching A layer from MAX phases. MAX phases are transition metal Carbides/Nitrides with a general formula of $M_{n+1}AX_n$, where M refers to early transition metal (such as Sc, Ti, V, Zr, Hf, Nb, Cr, Ta, Mo, etc.), A denotes the element from group III-A or IV-A and X denotes carbon/nitrogen. MAX phases have layered structure and 2D MXene sheets are also structurally similar to Graphene, because of this MXene name was given to this newly discovered family of 2D materials (Ihsanullah, 2020).

2.7.1 Structure of MAX Phase and MXene

MXenes have a similar hexagonal crystal structure to the parent MAX phase. The general formula for MAX phases is Mn+1AXn, where n typically varies from 1 to 3, resulting in M2AX (211), M3AX2 (312), and M4AX3 (413) phases, as shown in Figure 4a. In all the MAX phases, the "M" transition metal atoms form the octahedra and "X" atoms reside in these octahedra formed between the layers of "M" atoms, forming M_6X interleaved with the layers of "A" elements. The only difference between the 211, 312 and 413 phases is the number of M layers between two consecutive A layers (Sokol et al., 2019). In these MAX structures, there are two distinct M sites; M (1) that are adjacent to A and M (2) that are not adjacent to A layer. In short, the MAX phases consist of alternating layers of MX and A. Figure 4b illustrates a high-resolution TEM image of a MAX phase that appears "zig-zag" stacked and twinned due to the presence of two MX layers with the A layer acting as a mirror between them (Mathis et al., 2021). MAX phases have a hexagonal crystal structure having two formula units per unit cell with P63/mmc symmetry, as shown in Figure 4**c.** MAX phases are anisotropic with c lattice parameter of around ~ 13 Å for 211 phase, ~ 18 Å for 312

phase and ~ 23-24 Å for 413 phases. When an MXene layer is removed from MAX phase via etching, the remaining M layers having X elements in their octahedral sites are called 2D MXenes. These MXenes are mono transition metal MXenes, but chemically ordered MAX phases containing them were only discovered recently, more than one M element having in-plane ordering in 2014 (Hadi et al., 2018)**,** and out-of-plane ordering in 2017 (Gonzalez-Julian, 2021), the double transition metal MXenes and divacancy MXenes with ordered structure have been developed..

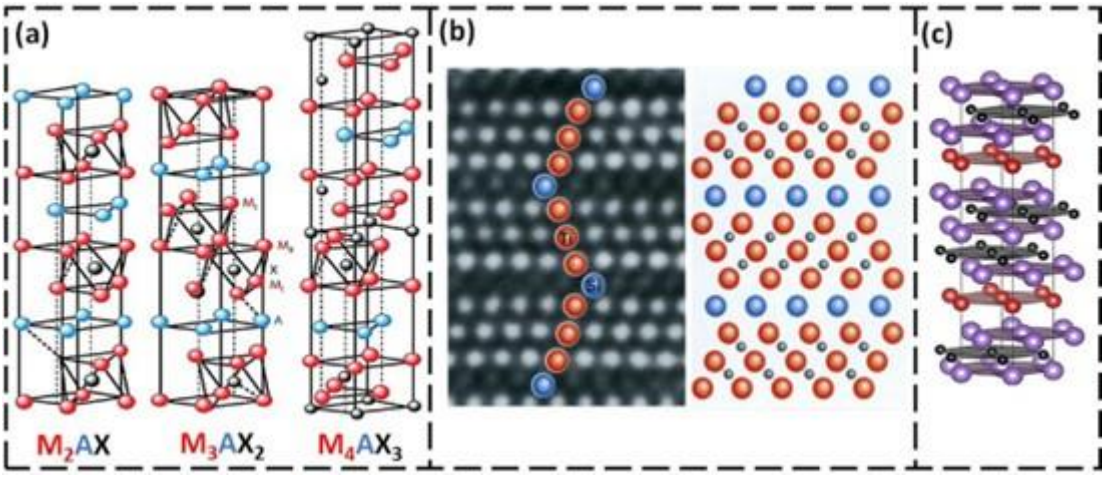

Figure 4: Crystal Structure of different MAX Phases

2.8 Mxene for Water Treatment

Various types of MXenes are employed for water treatment applications including heavy metal ion removal, Dyes removal and desalination. MXene as an adsorbent, with its unprecedented performance in water remediation, superseded graphene, and other adsorbents. Here we will briefly discuss the employment of MXene for the removal of heavy metal ions and organic Dyes from wastewater.

2.8.1 MXene for Heavy Metal Ion Removal

Heavy metal ions such as Pb^{2+}, Cu^{2+}, Hg^{2+}, Ba^{2+}, etc. are dangerous to human health even at very low concentrations. MXene with high surface area, abundant adsorption sites and affinity toward metal capturing is a promising candidate for removal of toxic metal ions from water. So far, several researchers reported successful sequestration of heavy metal ions from water using MXene as an adsorbent. Some of these studies are discussed below.

2.8.1.1 MXene for Lead (Pb) Removal

The addition of lead to water is usually ionic (Pb2+). Lead, a toxic heavy metal, is prevalent in a variety of industries, including oil refining, lead-acid batteries, and construction materials. MXene, a novel, lightweight, effective, and environmentally friendly material, has the potential to be used for the removal of Pb(II) from water through electrostatic adsorption and exchange. MXene and Chitosan was used on the PU foam as a support materials and breakthrough curves were observes. Different adsorbents based on the coating were studies and 80% of lead removal was observes in first 20 minutes of operation (Shafiq et al., 2021). Despite having a surface area of powder activated carbon (~470 m^2/g) that was ~50- fold higher than that of MXene (10 m^2/g), MXene also exhibited better elimination capacity due to its higher negative surface charge (Jun et al., 2019).

2.8.1.2 MXene for Mercury (Hg) Removal

Mercury (Hg) is a water-soluble and highly toxic heavy metal. Hg could cause several health-related issues, such as kidney illnesses, chromosome alteration, birth defects and damage to the central nervous system. Major sources of mercury are cement factories, gold mining industries, paint industries, electronic home appliances and Chromium acid batteries etc. To address this issue, Shahzad et al. reported sodium alginate functionalized MXene and prepared $Ti_3C_2T_x$-filled spheres containing sodium alginate (MX-SA) with ultrahigh capturing (932.84 mg g^{-1}) of mercuric ions. Functional groups like carboxyl(-COOH), hydroxyl(-OH) & alkanes(-CH) of biopolymer alginate performed a crucial role in heavy metal. The formation of new binding groups like [Ti−O]−Ca+ and [Ti−O]−H+ in MX-$SA_{4:20}$ was also predicted to have strong interaction with Hg^{+}. Shahzad et al. also integrated MXene ($Ti_3C_2T_x$) sheets with nanolayered MoS_2 for capturing toxic mercuric ions Hg^{+2} at the pCr level and showed its high stability in water and demonstrated the prepared adsorbent as recyclable. Sulfur atoms from MoS_2 and O from MXene played a crucial role in the sequestration of mercuric ions and it was shown that Adsorption occurred as a result of the formation of Hg-S and Hg- O complex binding (Shahzad et al., 2018).

2.8.1.3 MXene for Barium (Ba) Removal

Barium is also water soluble and can cause difficulty in breathing, increase in blood pressure, muscle weakness, changes in nerve reflexes, heart rhythm changes, stomach irritation, liver and brain swelling, and heart and kidney damage. To address

this issue, Fard *et al.* conducted an adsorption study for Ba^{2+} ions using Ti3C2Tx adsorbent (Fard et al., 2017). They achieved 9.3 mg g^{-1} adsorption capacity with an initial metal ion (Ba^{2+}) concentration of 55 ppm at pH 6-7. Fard and co-workers reported high selectivity of Ti3C2Tx MXene (presence of -OH groups on the MXene surface) towards Ba^{2+} removal in a solution containing multiple metal ions. Jun et al. also studied MXene for Ba^{2+} ion removal and achieved an adsorption capacity of 75.1 mg g^{-1} in a 2gL^{-1} Ba solution using 1gL^{-1} MXene ($Ti_3C_2T_x$).

2.8.1.4 MXene for Copper (Cu) Removal:

Copper ions can be removed from contaminated water using MXene. Dong et al. used an MXene/alginate composite to remove copper from wastewater. (Dong et al., 2019b). 382.7 mg g−1 of copper was adsorbed in the presence of Cu2+ (Dong et al., 2019b). The adsorption process was accelerated by MXene/alginate as well as enhanced by copper (Dong et al., 2019b). Cu ions are captured on MXene/gelatin through both chemical coordination and ionic exchange (Dong et al., 2019b). The Levodopa (DOPA), an amino acid, was successfully functionalized on MXene surfaces using self-polymerization. Cu2+ ions were adsorbed by carboxyl groups that were induced on the surface of MXene through chemical self-polymerization. Moreover, the Ti3C2TX-PDOPA composites (Gan et al., 2020)were used for Cu2+ adsorption, showing much higher adsorption than the unmodified $Ti_3C_2T_X$.

2.8.1.5 MXene for Dye Removal

Every year, more than 700,000 tons of 10,000 unique dyes are produced for use in a variety of industries, primarily textiles. Dyes are extremely poisonous and carcinogenic, which causes them to be extremely harmful to aquatic ecosystems. Due to their stable molecular framework, dyes are difficult to biodegrade. Due to the fact that adsorption is the most economical and efficient dye removal technique, it is the most widely used. There are many reports in the literature about the removal of organic dyes from wastewater using MXenes (Xu et al., 2022).

CHAPTER 3

MATERIALS AND METHODS

3.1 Materials

MAX phase (Ti_3AlC_2, Carbon-Ukraine Ltd.) with a particle size of < 40µm, Lithium Fluoride (LiF, Rieden-de Haen, Assay 99%) and HCl (37% reagent grade) were procured from Scharlau Chemicals. Glacial acetic acid (99%), Potassium dichromate ($K_2Cr_2O_7$) powder (Assay> 99.5%), and 1,5-Diphenylcarbazide (DPC) reagent were procured from DaeJung Chemicals, South Korea. Polyurethane Foam (White color) of the commercial grade was purchased from the local market. Yellowish powdered Chitosan was purchased from Solarbio, Beijing, China with a degree of acetylation of > 75%. All the solutions were prepared with high-purity deionized water (DIW) and experiments were carried out with laboratory-scale distilled water(DW).

3.2 Experimental Section

Experimental section consists of four steps:

- Adsorbent ($Ti_3C_2T_x$ MXene) synthesis
- Dip coating PU Foam with $Ti_3C_2T_x$ Adsorbent
- Characterization of $Ti_3C_2T_x$ and $Ti_3C_2T_x$ coated PU foam
- Adsorption test of PU Foam coated with $Ti_3C_2T_x$

Schematic of the experimental section is represented in Figure 5:

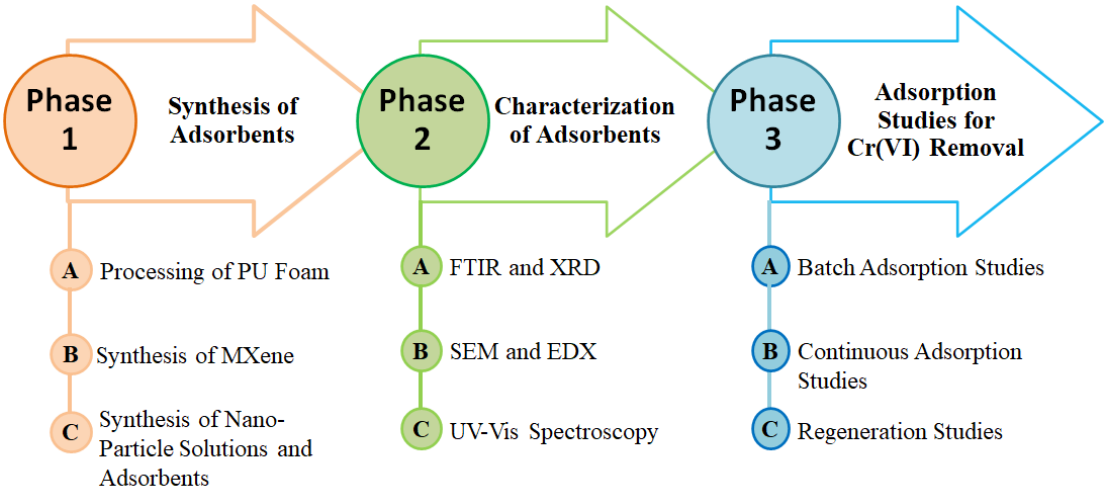

Figure 5: Schematic diagram for the research study

3.3 Synthesis of Ti3C2Tx MXene From MAX Phase (Ti_3AlC_2)

$Ti_3C_2T_x$ MXene was synthesized by selective etching of the Al element from Ti_3AlC_2 MAX phase via in-situ hydroflouric acid (HF) formation. For Etching 2g of MAX Phase (Ti_3AlC_2) , 2.66g Lithium Flouride (LiF) (Ti_3AlC_2 : LiF = 1:10 Molar ratio) was mixed with 40ml of 9M HCl in a polypropylene bottle with constant stirring for 5-10 minutes for HF formation, and then Ti_3AlC_2 powder was added slowly to the mixture of LiF and HCl under constant stirring for 5 minutes to avoid excessive heat and gas bubbles formation in the bottle. After completely adding Ti_3AlC_2, the mixture was kept under constant stirring at 35ºC for 24 hours. After 24 hours of reaction time, a black solution of MXene ($Ti_3C_2T_x$) was obtained, which was washed several times with deionized water until the solution reached pH ~ 5.5-6. For each washing cycle, the transparent supernatant is discarded, and fresh DI water is added for the next washing cycle. As the pH is reached the desired value as mentioned above, $Ti_3C_2T_x$ is collected by adding DI water and shaking for 30 seconds. The first collected sample is expected to be the ink of single-layer 2D $Ti_3C_2T_x$ nanosheets. Further collection by adding DI water and shaking for 30 seconds yields a mixture of single and multilayered 2D $Ti_3C_2T_x$ nanosheets. A schematic of $Ti_3C_2T_x$ MXene synthesis by etching of Ti_3AlC_2 MAX phase is shown in Figure 6 (Yu et al., 2022).

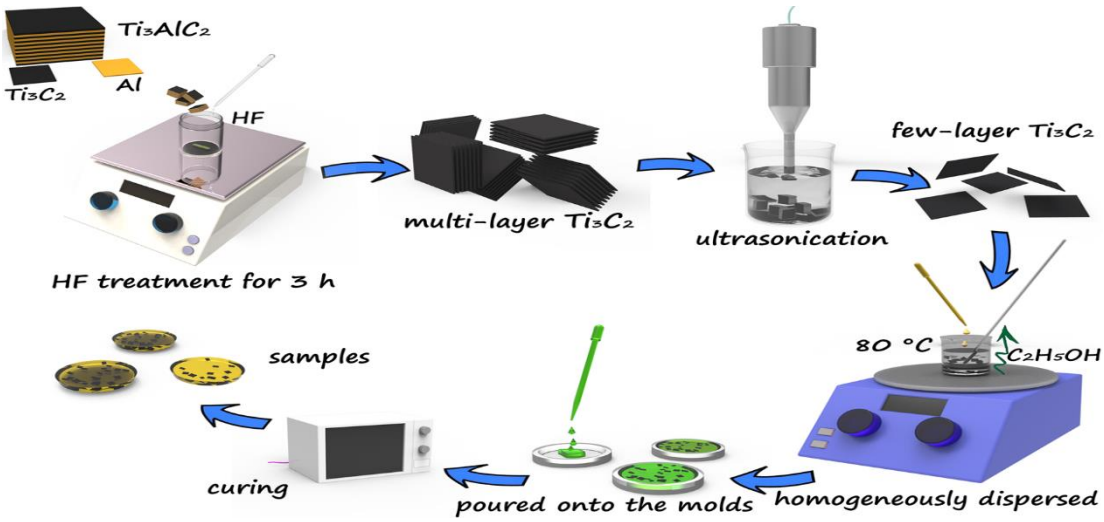

Figure 6: Synthesis of MXene (Ti_3C_2Tx) from MAX Phase (Ti_3AlC_2)

3.4 Synthesis of PUF Adsorbents Coated Chitosan/MXene ($Ti_3C_2T_x$)

PU foam was cut into 1x1x1 cm^3 size samples and washed 3 times with DI water and ethanol respectively. After washing, these samples were dried in the oven at 60ºC temperature for 4 hours. After the drying is completed, 10 samples of dried Pristine PU

foam (PUF) were separated and the remaining samples were dipped in a 0.4 wt% (4mg/ml) chitosan solution, squeezed several times until the foams were completely soaked with chitosan solution. After soaking, the 2 minutes of residence time was given in Chitosan solution. After 2 minutes the foams were squeezed to remove extra chitosan just absorbed by the PU foam skeleton and dried in the oven at 60ºC for 4 hours. After the drying is completed, 10 samples of dried chitosan-coated PU foam (CH@PUF) were separated and the remaining CH@PUF samples were dipped in 4.5 mg/ml $Ti_3C_2T_x$ solution, squeezed several times until the CH@PUF samples are completely soaked by $Ti_3C_2T_x$ solution. After a residence time of 20 minutes in $Ti_3C_2T_x$ solution, CH@PUF samples were squeezed to remove extra $Ti_3C_2T_x$ just absorbed on the skeleton of CH@PUF and dried in Oven at 60ºC for 4 hours. After drying, 10 samples of CH@PUF coated with $Ti_3C_2T_x$ (named M_1@CH@PUF, where 1 denotes the no. of layers of $Ti_3C_2T_x$) were separated. The remaining 10 samples of M_1@CH@PUF were again coated with chitosan and $Ti_3C_2T_x$ for two more layers of each CH and $Ti_3C_2T_x$, using the same approach as described above (2 minutes in CH and 20 minutes in $Ti_3C_2T_x$ solution). After coating 3 layers of CH and $Ti_3C_2T_x$, the 10 samples (MX_3@CH_3@PUF) were separated. Pristine PU foams with the same dimension mentioned above were also dip-coated directly with $Ti_3C_2T_x$ without using CH. For this purpose, 10 samples of Pristine PU were dipped in $Ti_3C_2T_x$ solution, after squeezing several times in $Ti_3C_2T_x$ solution until the foams are completely soaked, foams are left in the solution for a residence time of 20 minutes. After that, foams are squeezed to remove extra $Ti_3C_2T_x$ solution absorbed in the skeleton and then dried in the oven at 60ºC for 12 hours. After drying, MX_1@PUF samples are obtained. 10 samples were separated and the remaining 10 samples of MX_1@PUF were again coated with the same method as mentioned above up to 3 layers of $Ti_3C_2T_x$. samples coated with 3 $Ti_3C_2T_x$ layers without chitosan (MX_3@PUF) are separated for further use in fixed bed column studies.

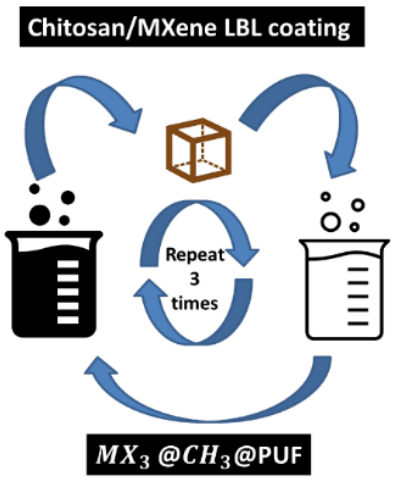

Figure 7: Illustration of Polyurthane foam coating process with MXene and Chitosan

3.5 Characterization of MXene and Coated PUF Adsorbents

Coating nanomaterials and synthesized PUF adsorbents were characterized by number of analytical techniques to evaluate the coating effectiveness on polyurthenae foam as a adsorbent. Following section describes the experimental procedure with some theoretical background for each technique.

3.5.1 X-Ray Diffraction (XRD)

X-ray diffraction (XRD) is a powerful technique, used to analyze crystalline phases of materials. It works on the principle of constructive interference, where monochromatic X-rays interact with a sample such that the incident beam angle is the same as the diffracted beam (the major condition to follow Bragg's law $n\lambda=2d\sin\theta$) and provide the peak intensities based on the atomic arrangement within the lattice. In this study, Crystal structures were analyzed by X-ray diffractometer (θ-θ STOE Germany). Diffractograms were acquired with continuous scanning from 5 to 80^o (2θ) with a step size of 0.04^o (2θ). The crystallinity of all the samples were calculated by using the equation below;

$$\text{Crystallinity} = \frac{\text{area of crsytalline + amorphous peaks}}{\text{Total area of crsytalline + amorphous peaks}} \text{ X } 100$$

Phase identification was measured using X`Pert High Score Plus software. The degree of crystallinity was determined based on characteristic peak`s intensity at 2θ.

3.5.2 SEM- EDS Analysis

In Scanning electron microscopy (SEM) highly focused electron beam falls on the sample surface and interacts with the sample's atom. In this study, surface

morphology of the nanomaterial and prepared adsorbents were analyzed by scanning electron microscopy along with energy dispersive spectroscopy (Joel JSM-6490A, Japan). To acquire the SEM images the acceleration voltage was set as 20 kV. And different magnifications i.e., 10X, 30X, 50X, 100X, 1000X was used.

3.5.3 Fourier Transform Infrared Spectroscopy (FTIR)

FTIR spectroscopy works under the infrared range and deals with the vibrations of the molecules. This technique is used for the analysis of polymeric, organic, and often for inorganic materials. Every molecule has a different response in terms of its vibration and bending movement which interacts differently with infrared light and produces a specific signal. This signal helps identify the type of molecule present in the materials. In this study, Functional groups on the surface of adsorbents were determined by using Fourier infrared spectroscopy (FTIR; Bruker Spectrum 400 spectrometer). The KBr disk method was used for this purpose having wavenumber ranged from 4000 to 400 cm^{-1}, with a resolution of 1 cm^{-1}.

3.6 Adsorption Experiments

The Cr (VI) stock solution (1000 mg/L) was prepared by dissolving potassium dichromate ($K_2Cr_2O_7$) in distilled water.

3.6.1 Batch Adsorption Experiment

Batch equilibrium tests were carried out for adsorption of Cr (VI) on the adsorbent prepared. Adsorption studies were carried out using Erlenmeyer flasks (250 ml) with glass stoppers. The freshly prepared solutions of adsorbate having different initial concentrations were placed in these flasks (Zeng et al., 2021). A definite amount of prepared adsorbents were placed on the flasks and kept inside a mechanical shaker for a definite period of contact time. The effects of initial adsorbate concentration, adsorbent dosage, and solution pH at a constant agitation speed of 200 rpm for adsorption uptake and percentage removal were investigated. 0.1 gm of the adsorbent was added with a 100 ml solution of differently concentrated chromium solutions at pH 2.5 to check the adsorption ability. After the solutions achieve equilibrium, the concentrations were measured using UV-Vis Spectrophotometer (Specord 200, Anlytikjena, Germany). Different adsorption isotherm and kinetic models are used to study the removal of heavy metal ions from heavy metal effluent(Feng et al., 2021).

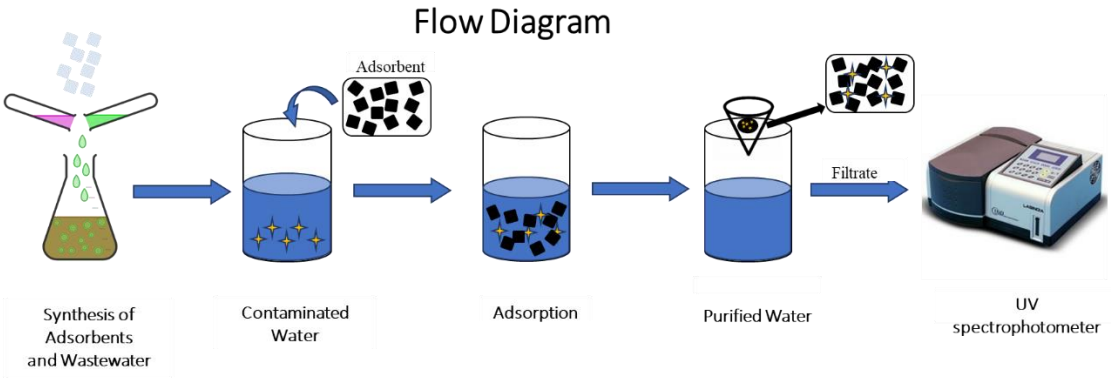

Figure 8: Schematic of Batch adsorption studies

3.6.1.1 Selection of Efficient Adsorbent

To select the most efficient adsorbent, adsorption experiments were carried out by shaking 0.1 g of adsorbent with 100 mL of Cr (VI) solution at 150 rpm. The initial concentration of Cr (VI) was 20 mg/100 mL. After filtration, the final concentration of Cr (VI) was determined by UV-Spectrometer (Specord 200 plus Germany). Removal efficiency (%) and adsorption capacity (mg/g) of the adsorbent was calculated as

$$\text{Removal Efficiency } (\%) = \frac{(C_o - C_e)}{C_o} * 100 \quad (2)$$

$$Q_e = (C_o - C_e) \times \frac{\text{Volume of solution}}{\text{mass of adsorbent}} \quad (3)$$

where C_o (mg/L) and C_f (mg/L) represent the initial and final concentration of Cr (VI) respectively. V (L) is the volume of solution and m is the mass of adsorbent.

After the selection of an efficient adsorbent, batch experiments were performed on the efficient adsorbent to optimize the experimental parameters i.e., adsorbent dosage, pH, contact time, initial concentration, and temperature.

3.6.1.2 Experimental Parameter Optimization

To optimize the experimental parameters for the removal of Cr (VI), all the parameters were varied one by one keeping the other parameters constant.

Effect of adsorbent dosage was determined by varying the dosage from 0.5 to 9 g/L. Other parameters include initial concentration of Cr (VI) 100 mg/L, pH 2.5, contact time of 120 minutes, temperature 25 ^oC and RPM 200.

Effect of pH was investigated by varying the pH value from 1.5 and 9. Other parameters include the initial concentration of Cr (VI) 20 mg/L, adsorbent dosage 2.5 g/L, contact time of 120 minutes, temperature 25 ^oC and RPM 200.

Effect of contact time varied from 0 to 360 minutes during which samples were analyzed at different time intervals (5, 15, 30, 60, 90, 120, 180, 240, 300, and 360 minutes). Other parameters include the initial concentration of Cr (VI) 20 mg/L, adsorbent dosage 2.5 g/L, pH 2.5, temperature 25^{o}C and RPM 200.

3.6.1.3 Adsorption Kinetic Studies

To quantitatively assess the trap of Cr (VI) by adsorbent, two well recognized kinetic models, i.e., Pseudo-first order (PFO) kinetic model and Pseudo-second order (PSO) kinetic model were used

$$qt = qe(1 - e^{-k1t}) \quad (4)$$

$$qt = q_e^2 k_2 t / 1 + q_e k_2 t \quad (5)$$

in which q_e (mg/g) and q_t (mg/g) represent the amount of Cr (VI) adsorbed at equilibrium and at time t, respectively. K_1 (min^{-1}) and k_2 (g/mg/min) are the respective rate constants.

3.6.1.4 Adsorption Isotherm Studies

Two well-known isotherm models, i.e., Langmuir Isotherm model and Freundlich Isotherm model were employed to quantify the adsorption data. These models predict the single and multilayer adsorption respectively.

$$qe = q_{max}. K_L. Ce / 1 + K_L Ce \quad (6)$$

$$qe = K_F Ce^{1/n} \quad (7)$$

in which q_{max} (mg/g) represents the uptake capacity of adsorbate onto the adsorbent. K_L represent the energy constant, $1/n_F$ is the coefficient related to sorption intensity, and K_F is the coefficient correspond to adsorption capacity (mg/g).

3.6.2 Fixed Bed Column Adsorption Experiment

Column studies are used to treat bulk amounts of wastewater with high yield, easy operating procedures, and simple design. Among all other column studies, Fixed bed column is well recognized and widely used method due to its excellent cyclic performance. In fixed bed column, a 100ml glass burette with a diameter of 1.5cm and height of 2 feet is packed with with the desired adsorbent with glass beads to the height needed by weighing the glass beads and then packing them in the columns (Laureano-Anzaldo et al., 2021). Contaminated water is circulated through these tubes with a

controlled flow rate adjusted with the help of a peristaltic pump. After passing through the adsorbent with a certain contact time, water is collected from the bottom of the tube and analyzed to check the reduced concentration of contaminants. The concentration vs time plot is given by a S-shaped breakthrough curve (C/C_0), which is the most important component of the adsorption studies via fixed-bed column (Shahzad et al., 2019).

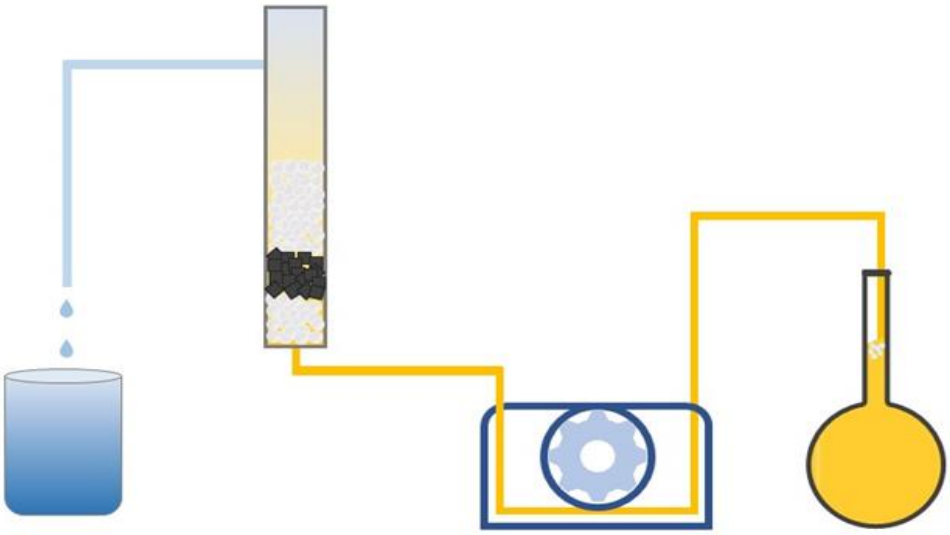

Figure 9: Schematic diagram of Column adsorption studies

3.6.3 Regeneration Studies

Regeneration experiments were also implemented after adsorption of Cr (VI) onto the adsorbent. The Cr (VI) packed adsorbent was compiled by filtering the adsorption experiment suspension and then placed in 1M NaOH solution for desorption while being meticulously stirred for 40 minutes. After stirring, the adsorbent was separated from the NaOH solution and washed numerous times with distilled water before being dried overnight. Adsorption experiments were performed as described earlier. The adsorption-desorption experiments were performed several times.

CHAPTER 4

RESULTS AND DISCUSSIONS

4.1 Characterization of MXene (Ti3C2Tx) and Adsorbents

The chapter presents the characterization and experimental results of all the adsorbent samples. The physical and chemical properties of the prepared adsorbents are determined.

4.1.1 SEM – EDX Analysis

The morphologies of pristine and coated polyurethane foam were examined using scanning electron microscopy. Elements present on the surface of adsorbents were also examined using EDS. The morphologies of pristine PU foam, anchored with Chitosan nanoparticles through dip coating and 3 layer by layer Ti3C2/chitosan coated PUF (MX_3@CH_3@PUF) before and after adsorption process are shown in Figure 10. The porous structure and interconnected skeleton of the clean pristine PUF were clearly showed in Figure 10(a). Surface of the uncoated pristine PU foam is smooth because of washing with the DI water and ethanol. Figure 10(b) reveals the internal structure of the chitosan coated PU foam (CH@PUF). It is observed that chitosan coating was done without deforming the internal structure of the PU foam. Furthermore, Figure 10(c) shows the coating of 3 LBL Ti3C2/chitosan on the PU foam (MX_3@CH_3@PUF) made the surface rougher and clearly exhibits the deposition of Ti_3C_2/chitosan on the lateral face of the PU foam before adsorption process. In Figure 10(d), the deformation of the PU foam internal skeleton was observed after the adosrption process which is the indication of adsorption process and influence of other parameters during the heavy metal removal process.

EDS is the technique used for the determinations of the elemental composition of a selected area and the relative elemental mass of synthesized adsorbents as shown in Figure 10. The achieved results confirmed that different elements present in the sample, such as nickel, iron and oxygen, while other elements like chlorine and sodium were also detected because the salt of the elements was used in the study as shown in Table 2. After Cr (VI) uptake, small particles were observed on the surface of MX_3@CH_3@PUF. These observations have been in line with the results of EDS where Cr(VI) anchored on the surface of MX_3@CH_3@PUF. Other common elements include C and O whereas trace elements of Ni and Cu are also present.

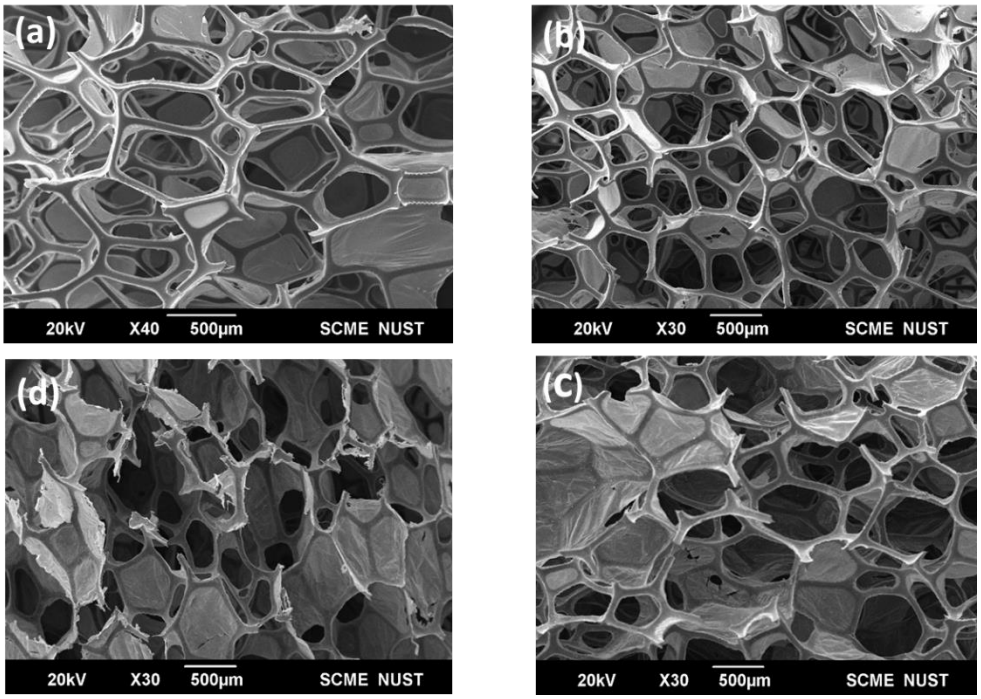

Figure 10: SEM analysis for (A) Pristine PU foam, PU foam anchored with different nanoparticles (b) Chitosan@PU foam, (C) MX3@CH3@PU foam (before adsorption),(D) MX3@CH3@PU foam (after adsorption) at different magnifications

Table 2:EDS of (a) MX3@CH3@PU foam (before adsorption) and (b) MX3@CH3@PU foam (after adsorption)

(a)

Elements	Weight (%)	Atomic (%)
C	48.1	64.4
O	22.8	22.9
F	5.1	4.3
Al	1.4	0.9
Cl	1.1	0.5
Ca	1.3	0.5
Ti	17.5	5.9
Ni	2.6	0.7

(b)

Elements	Weight (%)	Atomic (%)
C	34.6	49.2
O	33.3	35.9
F	3.9	3.5
Al	1.8	1.2
Cl	2.2	1.1
K	1.0	0.4
Ca	1.9	0.8
Ti	15.6	5.6
Cr	4.0	1.3
Cu	1.7	0.5

4.1.2 FTIR Analysis

To characterize surface functional groups on prepared $Ti_3C_2T_x$ and $Ti_3C_2T_x$ coated PU foams, FTIR spectroscopy was performed. MXene film was prepared from the same MXene which was used to coat PUF and small piece of Film and coated PUF was utilized for FTIR analysis. Figure 11 shows the FTIR spectrum of $Ti_3C_2T_x$, Pristine PUF, CH@PU, MX_3@CH_3@PU (Before adsorption) and MX_3@CH_3@PU (After adsorption) respectively.

For $Ti_3C_2T_x$, the broad peak at 3428 cm^{-1} is attributed to the stretching of the hydroxyl functional group (-OH) on the intercalated MXene surface. The presence of water molecules and hydroxyl group(-OH) on $Ti_3C_2T_x$ are confirmed by the bending vibration of H-OH at 1625cm^{-1}. The peak at 619 cm^{-1} is expected to be of stretching vibrations corresponding to Ti-O . The absorption peak at 1103 cm^{-1} refers to C-F stretching vibrations. Functional groups expected to be on MXene surface are also confirmed by the FTIR spectrum, affirming MXene to be an excellent adsorbent for heavy metal ions and other organic pollutants.

In Pristine PUF spectrum, Peak at 3393 cm^{-1} is ascribed to the stretching vibrations of N-H group. Peak at 2916 cm^{-1} was assigned to stretching of alkanes C-H with C=CH2 bond. Peak at 2314 cm^{-1} is of the asymmetric stretching of N=C=O. 1603 cm^{-1} peak in the spectrum is associated with the C=O stretching vibrations. Peak at 1324 cm^{-1} corresponds to C-C stretch of Alkane. The Broad peak at 1141 cm^{-1} is attributed to asymmetric vibrations(stretching) bands of C-O from N-CO-O group. Finally, the peak at 810 cm^{-1} represents C-H bond.

Chitosan-coated PUF has a similar spectrum to that of pristine PUF. MXene coated PUF (MX_3@CH_3@PU) Spectrum exhibited combined peaks of MXene and PUF. After adsorption of Cr (VI), -CO and -OH peaks are suppressed in the spectrum of MX_3@CH_3@PU because the surface of foam is covered with MXene layers and also, Cr (VI) ions are attached to most of the OH sites causing reduced peak intensity.

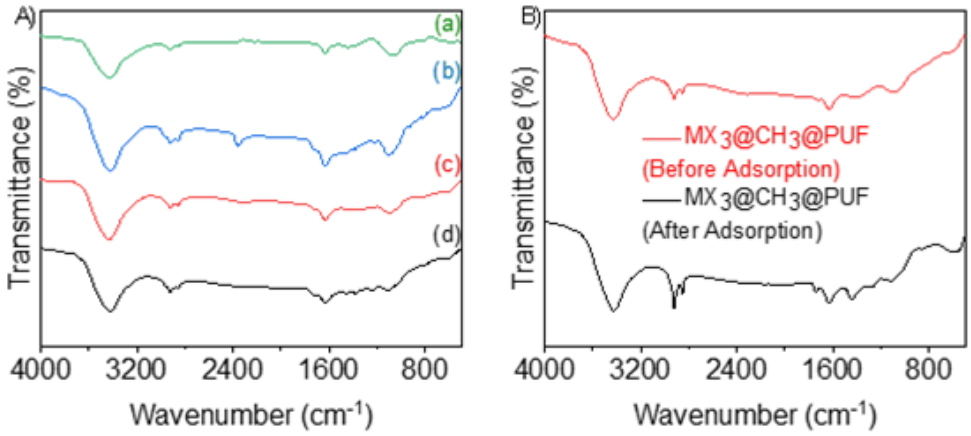

Figure 11: FT-IR spectra of (A-a) MXene (Ti3C2Tx),(A-b) Pristine PUF, (A-c) Chitosan@PUF and (A-d) MX@PUF (B) of potential adsorbent MX3@CH3@PUF before and after adsorption of chromium ions

4.1.3 XRD Analysis and UV-Vis Spectra

X-ray diffraction patterns of MXene and Chitosan are shown in figure 000. X-ray diffractometer (Theta/Theta STOE Joel Germany) with monochromatized Cu Ka was used to obtain X-Ray diffraction patterns of both of the compounds. The measurement was performed in the range from 5° to 80°. XRD spectrum of the prepared sample was investigated to confirm the formation of synthesized MXene and Chitosan nanoparticles. The major diffraction peak of MAX at 9.5° (002) is shifted to 7.1° in the exfoliated $Ti_3C_2T_x$ pattern indicating an expansion in the interlayer distance.

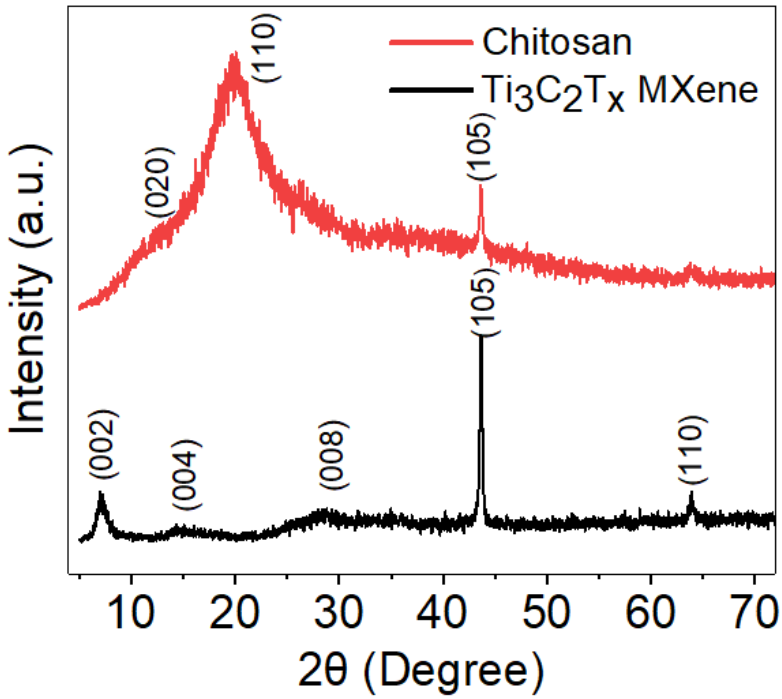

Figure 12: XRD Analysis of MXene and Chitosan

Where D is the crystallite size, β is the line broadening at the full width at half maximum (FWHM) of the most intense peak, K (0.9) is Scherrer constant, θ is the Bragg angle and λ is the X-ray wavelength. The average crystalline size of nickel ferrite nanoparticles was calculated as 30.254 nm. The average crystalline diameter (D) was calculated by Scherer's equation (8),

$$D=0.9\lambda/\beta\cos\theta \quad (8)$$

UV-Spectra of MXene colloidal solution is with a broad characteristic MXene peak at 270nm validating the synthesis of delaminated MXene (see Figure 13).

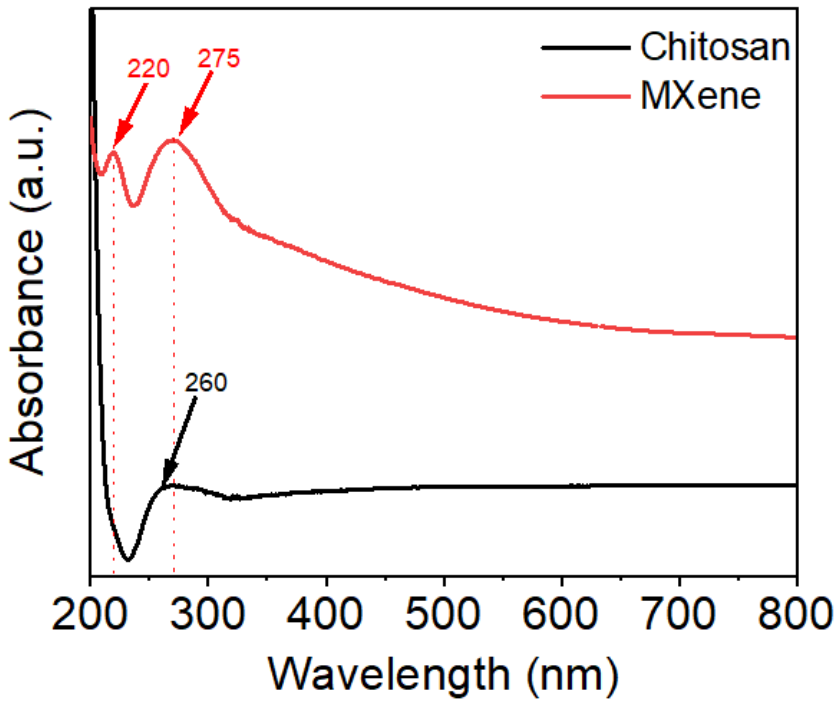

Figure 13: UV-Vis Spectra of MXene and Chitosan nanoparticles

4.2 Adsorption Experimental Results

4.2.1 Standard Calibration Curve for Cr (VI)

Diphenyl carbazide (DPC) standard method APHA 3500-CR was used for the detection of Cr (VI) using UV spectrophotometer. A red violet color indicates the presence of Cr (VI) ions in the solution. A calibration curve was prepared at λmax 540 nm using concentrations of Cr (VI) from 0.1 mg/L to 0.9 mg/L. Fig. 14 showed the calibration curve and the equation with a correlation factor R^2 0.9998.

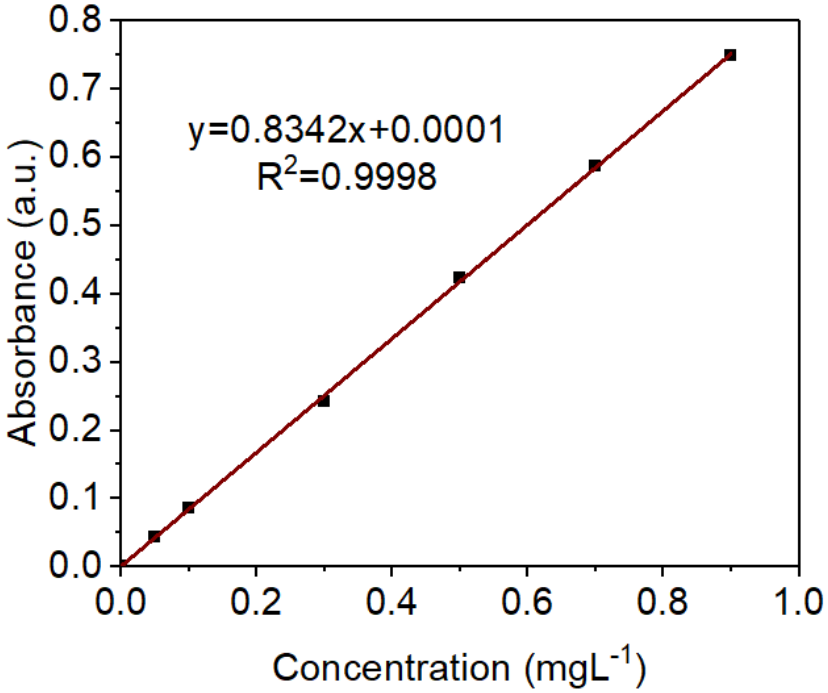

Figure 14: Calibration Curve of Chromium (VI)

4.2.2 Batch Adsorption Studies

The kinetic studies were performed using 250 ml volumetric flasks. 100 ml of 20 ppm Cr (VI) was taken in ten volumetric flasks each, 250 mg of pure MX_3@CH_3@PUF was added to each flask and then placed on an orbital shaker at 200 rpm, volumetric flasks were removed from the shaker after 120minutes. The solution left after was analyzed using UV Spectrophotometer (Spectrecord-Germany). The same process was repeated for the other adsorbents to find the optimum adsorbent for Chromium removal.

4.2.2.1 Selection of Efficient Adsorbent

To evaluate the appropriate adsorbent for Cr (VI) removal, different adsorbents were employed. The efficacy of these was assessed based on the Cr (VI) removal experiments taking the initial concentration of 10 mg/L at Ph 2 and 2.5 g adsorbent dose. Fig.000 exhibits the removal efficiencies of different adsorbents utilized. The removal efficiencies of pristine PUF, Chitosan@PUF (CPU), MXene@PUF (MPU), MXene(1 layer)@Chitosan (1 layers)@PUF (MC1PUF) and MXene(3 layer)@Chitosan (3 layers)@PUF (MC3PUF) are 29%, 42%, 59%, 73% and 85% respectively.

MX_3@CH_3@PU (MC3PUF) showed outstanding adsorption performance with 80% chromium removal at 25ºC in 2-hour operation. This high removal efficiency is due to high MXene loading on PUF as a result of strong electrostatic interaction of negatively charged MXene with positively charged chitosan on PUF surface.

The higher removal efficiency of MX_3@CH_3@PU is due to the higher surface area provided by the composite materials prepared by the chitosan and MXene coating. MXene provided extra strength to the PUF skeleton to uphold more chromium ions and stabilize its cubical structure. Also, because of chitosan, MXene layers were more uniformly attached to PUF as compared to that without chitosan (MX_3@PU). Therefore, MX_3@CH_3@PU showed high durability and >40% Chromium removal even after 3 hours of the continuous flow of Chromium-containing water. From this, we can speculate that MX_3@CH_3@PU with a weight of 20 g becomes saturated after treating 1000ml of water upto 80% efficiency (50 times more than its own weight).

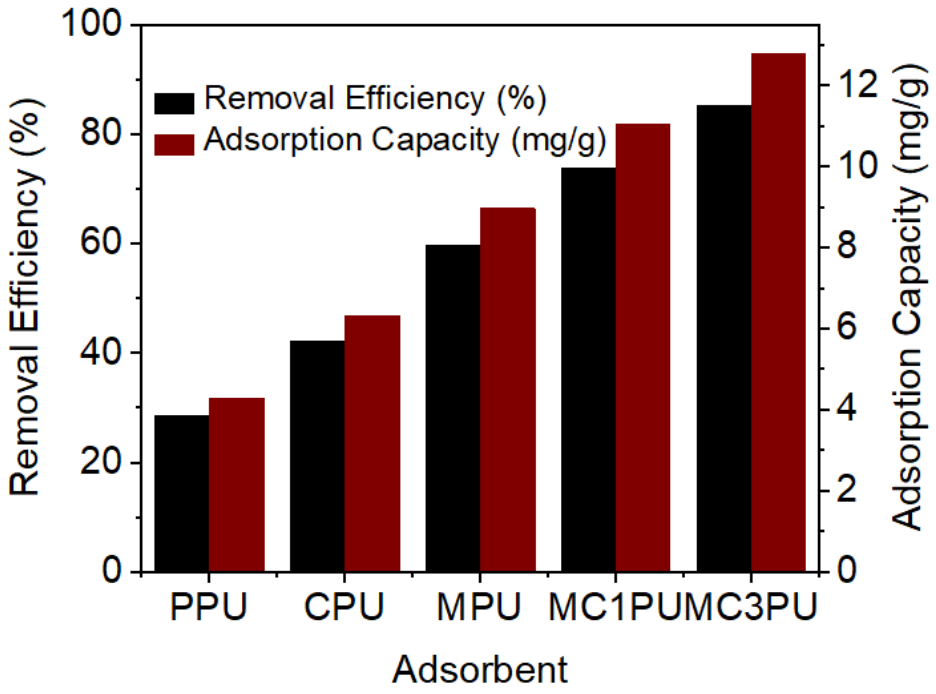

Figure 15: Types of different adsorbents used for Chromium (VI) removal.

4.2.2.2 Effect of Adsorbent Dosage

Adsorbent dose is a critical constraint influencing the adsorption capacity of an adsorbent under given adsorbate concentration and operating conditions. Figure 16 represents the removal efficiency and adsorption capacity of Cr (VI) on Adsorbent at different doses (0.3, 0.5, 1, 1.5, 2, 2.5, 3 g). As the adsorbent dose increases removal efficiency also increases whereas adsorption capacity is reduced.

This increment was assigned to more active sites and large surface area for high adsorbent doses. It was noticed that removal efficiency increased rapidly when the adsorbent dose increased from 0.5 g to 2.5 gL-1 as compared to 2.5 to 3 gL-1. In comparison adsorption capacity tends to decrease with an increase in adsorbent dose. This trend was attributed to the fact that for a particular initial concentration of adsorbate available sites and surface area was larger and the intensity of adsorbate loaded onto the unit surface area was lower.

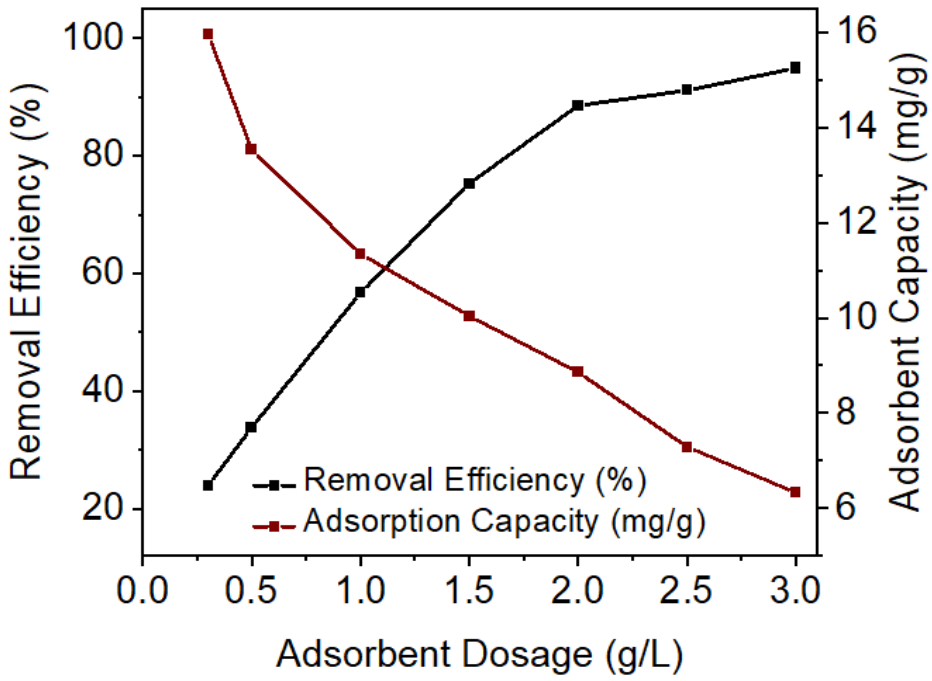

Figure 16: Effect of adsorbent dosage on Cr (VI) removal efficiecny and adsorption capacity

4.2.2.3 Effect of pH

It is evident from the Figure 17 that Cr (VI) ion pH is critical in adsorption study. To determine the optimum pH on which maximum adsorption is obtained the removal was observed on different pH values(1.5-9) by MX_3@CH_3@PUF. The removal efficiencies calculated were 95.63%, 96.11%, 87.34%, 65.35%, 34.73%, 30.69% and 25.74% at pH value 1.5,2,3,4.5,6,7.5 and 9 respectively. The results indicates that MX_3@CH_3@PUF uptakes higher ions at more acidic than alkaline pH. pH range 1.5-3 found the optimum and pH 2 is considered for the futher experimentations which is also indicated in many previous studies. Adsorption capacity showed a harmonized relation with the removal efficiency of ions at acidic pH range. Adsorption capacity decreases with the decrease in removal efficiency as moving towards alkaline pH.

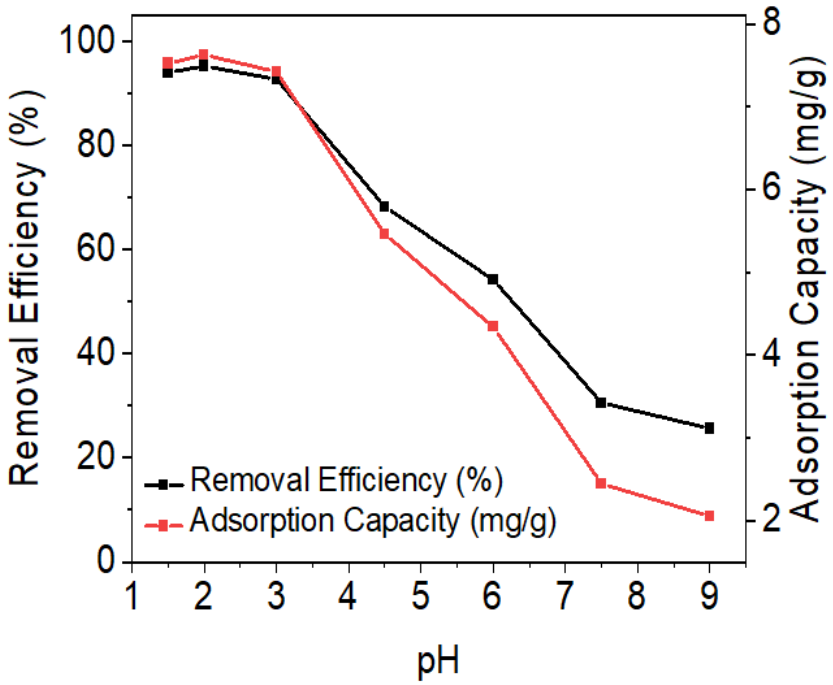

Figure 17: Effect of pH on Cr (VI) removal efficiency and adsorption capacity

4.2.2.4 Effect of Initial Ion Concentration

To evaluate the adsorption performance of the MX_3@CH_3@PU adsorbent, the initial Cr (VI) ions concentration was varied (5, 10, 20, 50, 100, 200 ppm). The influence of several initial concentrations of Cr (VI) on adsorption capacity is shown in Figure 18. It can be seen from the figure that adsorption capacity increased from 1.96 mg/g to 17.38 mg/g while removal efficiency(%) decreased from 98.35% to 22.11% with an increase in initial concentration of Cr (VI) from 5 mg/L to 200 mg/L. This increase in adsorption capacity results from higher pollutant i.e., Cr (VI) concentration, which offer higher driving force to overcome all mass transfer resistances, that ultimately result in high Cr (VI) adsorption.

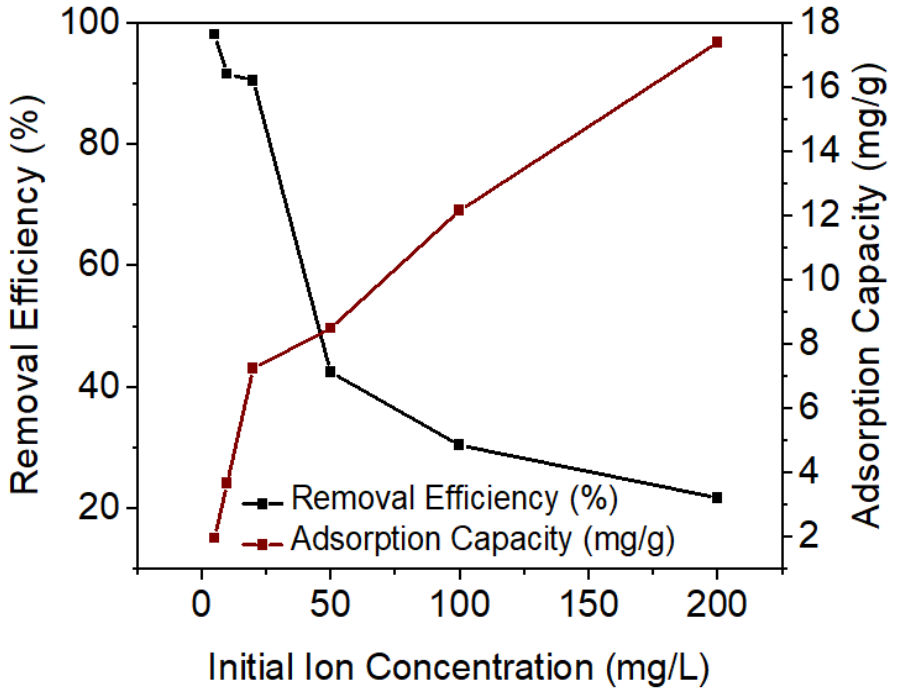

Figure 18: Effect of initial ion concentration on Cr (VI) removal efficiency and adsorption capacity

4.2.2.5 Adsorption Kinetic Studies

To quantitatively evaluate the adsorption kinetics and mechanism for adsorption the experimental data of adsorbetn was fitted by pseudo first order, and pseudo second order kinetic models. The fitted plots are shown in Figure 19. Adsorption process of 3 times coated PU foam was better fitted with pseudo second order kinetic model with correlation coefficient R^2 = 0.991 as compared to the pseudo first orderi.e., R^2= 0.990 for adsorbent. The calculated values of adsorption capacity (mg/g) were close to the experimental values as depicted from Table 3. Therefore, these results proposed the adsorption of Cr (VI) onto the porous adsorbent was subjugated by chemisorption by sharing or exchanging of electrons between adsorbents and Cr (VI).

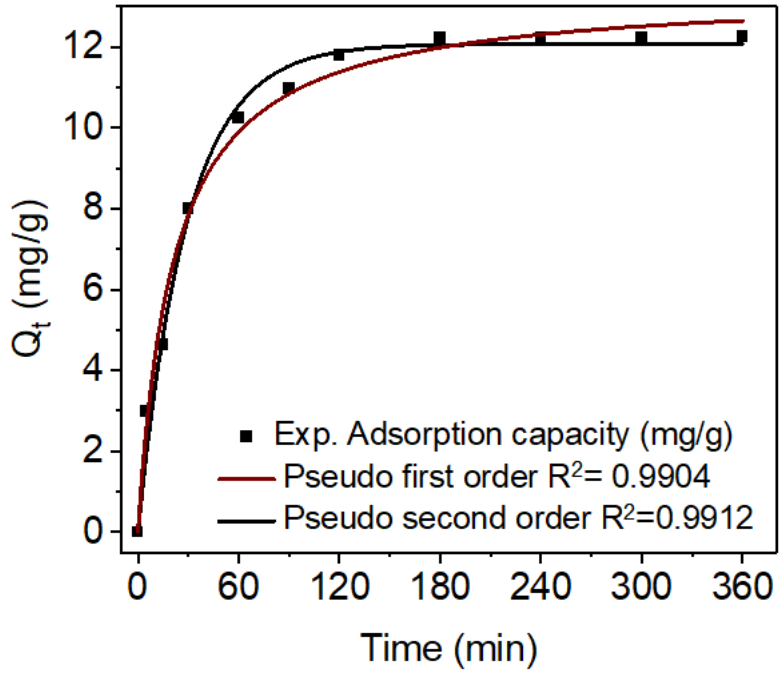

Figure 19: Adsorption kinetic model plot for Cr (VI) removal

Table 3: Kinetic model parameters for Cr (VI) adsorption

		Pseudo First Order Model			Pseudo Second Order Model		
Adsorbent	qe exp.	qe cal. (mg/g)	K_1 (L/mg.m)	R^2	qe Cal. (mg/g)	K_2 (g mg^{-1}. min^{-1})	R^2
MX_3@CH_3@ PUF	17.52	12.073	0.0344	0.990	13.401	0.0035	0.991

qe exp.= qe Experimental qe Cal.= qe Calculated

4.2.2.6 Adsorption Isotherms Studies

The Langmuir and Freundlich isotherm models were used to quantitatively analyze the adsorption performance of Cr (VI) by adsorbent (Figure 20). Data were fitted by nonlinear regression using Origin Pro 2021 Software. Results presented in Table 4 have shown that Freundlich isotherm model better describe the adsorption of Cr (VI) by MX_3@CH_3@PU with a higher correlation coefficient of R^2=0.932 as compared to Langmuir isotherm model R^2 = 0.757 under 25ºC temperature. Freundlich isotherm suggested that the uptake of Cr (VI) occurred on the multifaceted surface of adsorbent, succeeding in multilayer adsorption on the surface of binding sites between surface functional groups of MX_3@CH_3@PU and Cr (VI). The $1/n_F$ value of

Freundlich isotherm model was less than 1 and proposed that the adsorption of Cr (VI) onto the MX_3@CH_3@PU was favored by chemical adsorption.

Moreover, the maximum Langmuir uptake(q_{max}) of MX_3@CH_3@PU for Cr (VI) was estimated to be 17.38 mg/g at 25^oC which is comparable to other adsorbents previously reported as shown in Table 4.

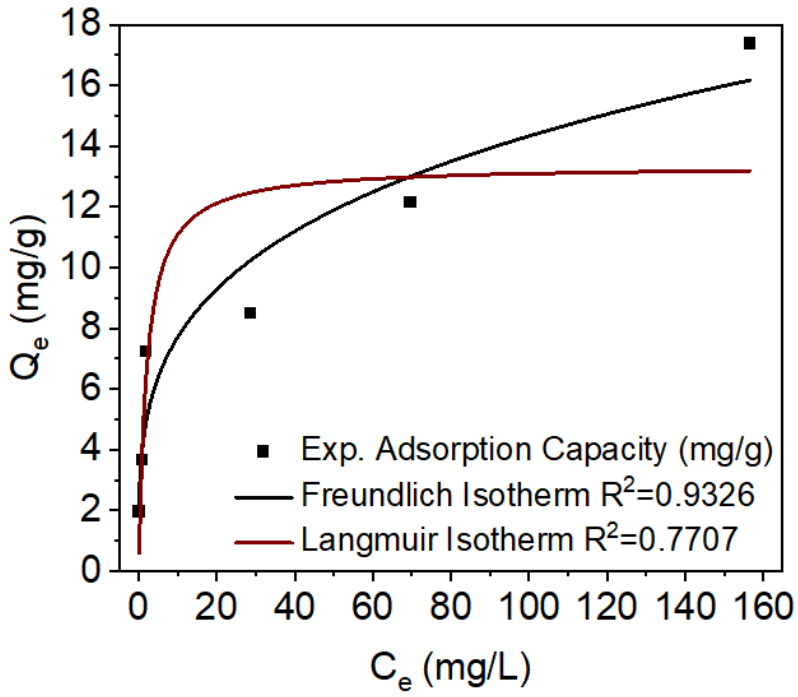

Figure 20: Adsorption Isotherm Model for Cr (VI) Removal

Table 4: Adsorption Isotherm Parameters

		Langmuir Isotherm			Freundlich Isotherm		
Adsobent	T (C^o)	q_{max} (mg/g)	K_L (L/mg)	R^2	$1/n_F$	K_F (mg/g) $(L/mg)^{-1}$	R^2
MX_3@CH_3@PU	25	13.562	0.378	0.757	0.298	3.629	0.932

4.2.2.7 Regeneration Studies

The reusability of the adsorbent is an important factor in determining its practical application in industry. Adsorption of Cr (VI) is highly pH dependent of the solution and difficult to desorb with acidic reagents**.** Results of Cr (VI) adsorption-desorption are depicted in Fig. 19 and indicate that removal of Cr (VI) using

regenerated MX_3@CH_3@PU maintained over 50% after first three cycles. While decreased to 18.24% after fifth cycle. Meanwhile the desorption efficiency was far less than that of adsorption. It decreased from 85.97% after first cycle to 18.24% after fifth cycle. Results concluded that strong chemosorption of Cr (VI) occur on the adsorbent surface. Decrease in adsorption-desorption efficiencies during each cycle could be due to the blockage of pores and hard desorption of complex between functional groups and Cr (VI), which ultimately reduce the active sites on the surface of adsorbent (Qu et al., 2021). Overall, results suggested MX_3@CH_3@PU to be dependable adsorbent and can be applied for practical application.

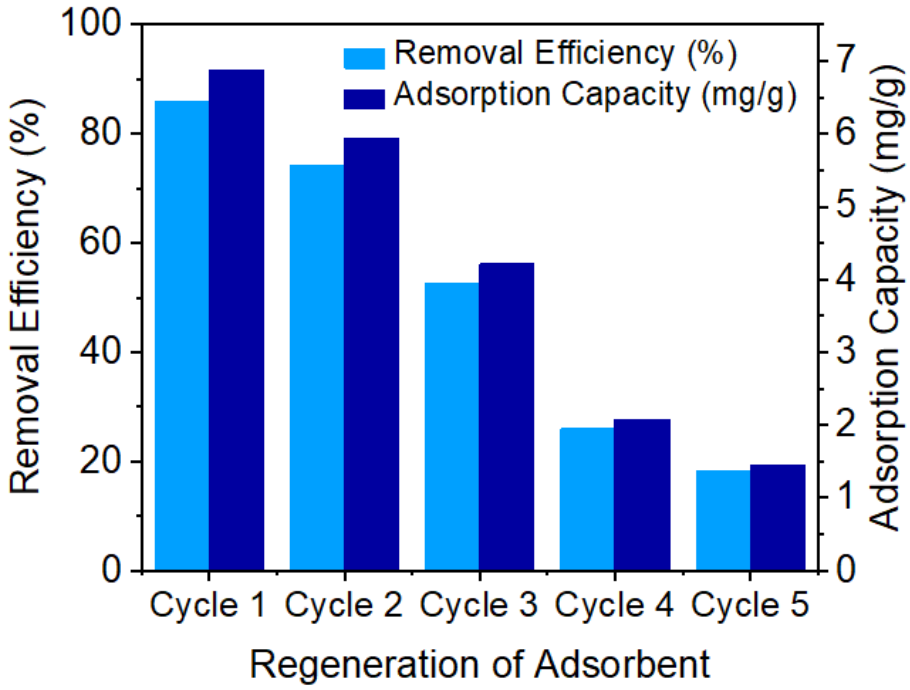

Figure 21: Regeneration performance of MX3@CH3@PU adsorbent

4.2.3 Fixed Bed Column Studies

Initial/influet concentrations of the adsorbate on breakthrough curves were analyzed. Regeneration and recycling efficiency of the column for MX_3@CH_3@PU are presented in the subsequent section.

4.2.3.1 Selection of Efficient Adsorbent

Adsorbents were packed in columns and continuously feeded with the synthetic effluent containing 10ppm Cr(VI) with a flow rate ~1mL/min^{-1}. Breakthrough curves for each of the samples are shown in Figure 22. Initially, Pristine PUF exhibited ~74% adsorption in the first 5 min, later its adsorption capacity gradually decreased over time, and ultimately desorption started after 130 minutes of operation. Chitosan@PUF (CH@PUF) on the other hand showed slow adsorption as compared to pristine PUF in the first 10 min, however, ~20% more saturation time was observed as compared to pristine PUF. The moderate increment in adsorption capacity was ascribed to the presence of suitable functional groups on chitosan which chelates the Cr(VI) ions. MX_3@PUF showed >70% Cr(VI) adsorption from continuously flowing effluent up to 20min and >55% chromium removal up to 40 min of continuous feed of Cr(VI) containing water.

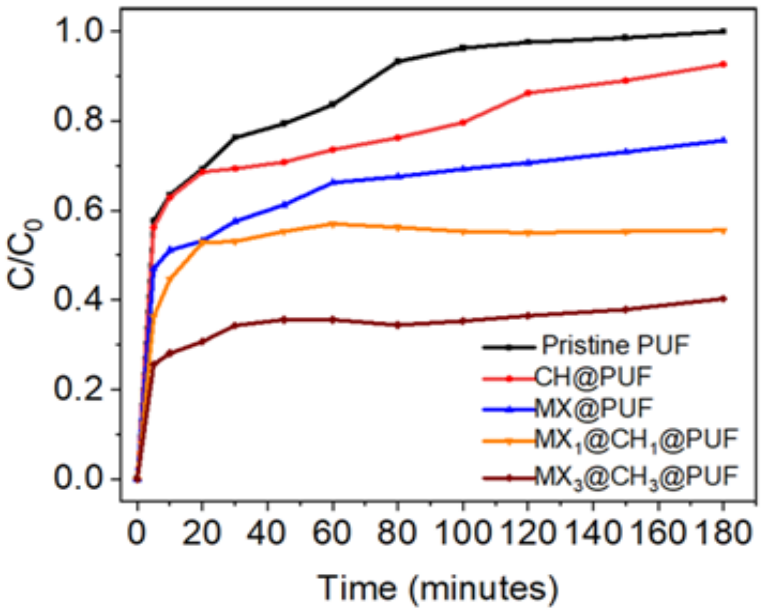

Figure 22: Breakthrough curve for Cr(VI) removal with different adsorbents

This enhancement in adsorption capacity was due to plentiful negative surface functional groups (--OH, --O) on the MXene(Ti3C2Tx) surface which captures Cr(VI) ions from water with strong electrostatic interaction. $MX_3@CH_3@PUF$ showed excellent adsorption performance with 80% Cr(VI) removal during initial 20 min and >50% removal after 2h. The high removal efficiency was caused by the strong electrostatic interactions between negatively charged MXene and positively charged chitosan on PUF that resulted in high MXene loading. A continuous flow of Cr(VI) contaminated effluent was able to remove >40% of $MX_3@CH_3@PUF$ after 6 hours.

4.2.3.2 Effect of pH

The initial pH value of the solution is of great importance in the adsorption performance due to the fact, pH value affects the surface charge of PU foam and forms of Chromium ions. The effect of aqueous pH on the adsorption of hexavalent chromium onto $MX_3@CH_3@PUF$ was studied by varying the range of pH from 2.5 to 6. Figure 23 shows the effect of pH on the adsorption behavior of MX3@CH3@PUF in a continuous process. The highest adsorption removal efficiency was observed at pH 2.5, where the salinity of the solution was highest. Due to the presence of Ti-O groups, ionic exchange and electrostatic interaction are the main adsorption mechanisms. Chromium ion removal efficiency decreases from 82% to 65% from pH 2 to 4 and 18% at pH 6. The degree of protonation of the functional groups on the adsorbent, the surface charge of the adsorbent, and the form of chromium in the adsorption system are all affected by the pH value.

When the pH ranged from 2 to 6, the main forms of chromium were $Cr^{3+,}$ $Cr^{2+,}$ $Cr_2O_7^{2-}$, and $HCrO_4$. Mainly chemical reactions in the solution were following;

$$Cr_2O^{2-}{}_7 + H_2O \rightarrow 2HCrO^{-}{}_4 \quad (9)$$

$$HCrO^{-}{}_4 \rightarrow CrO^{2-}{}_4 + H^+ \quad (10)$$

$$2CrO_4^{2-} + 2H^+ \rightarrow Cr_2O_7{}^{2-} + H_2O \quad (11)$$

$$Cr_2O_7^{2-} + 14H^+ + 6e^- \rightarrow 2Cr^{3+} + 2H \quad (12)$$

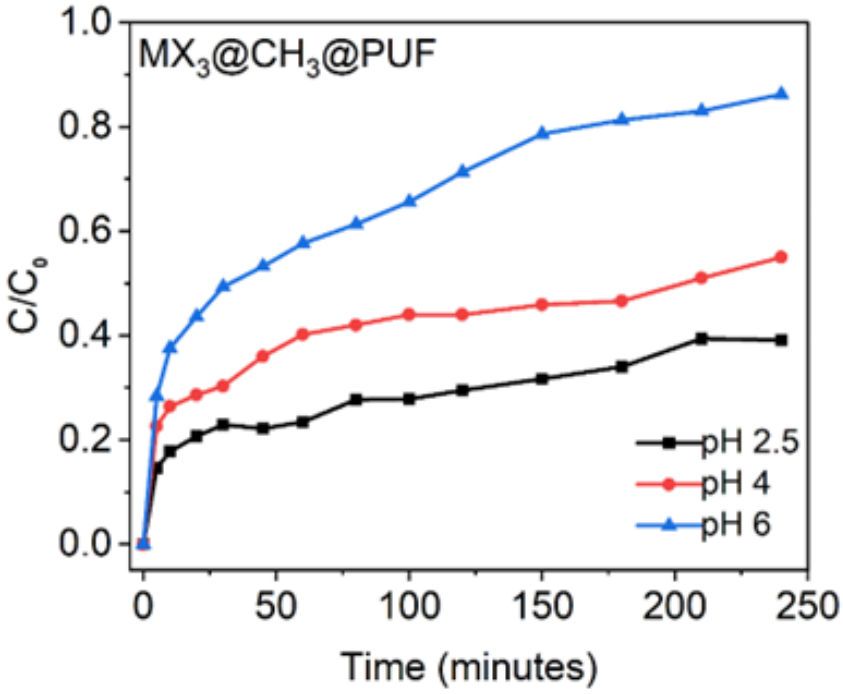

Figure 23: Breakthrough curve for MX3@CH3@PU with different pH for Cr(VI) removal

4.2.3.3 Effect of Initial Ion Concentration

To observe the adsorption performance of the adsorbent (MX_3@CH_3@PUF) the initial concentration of Cr(VI) was varied (10ppm, 20ppm, 50ppm).

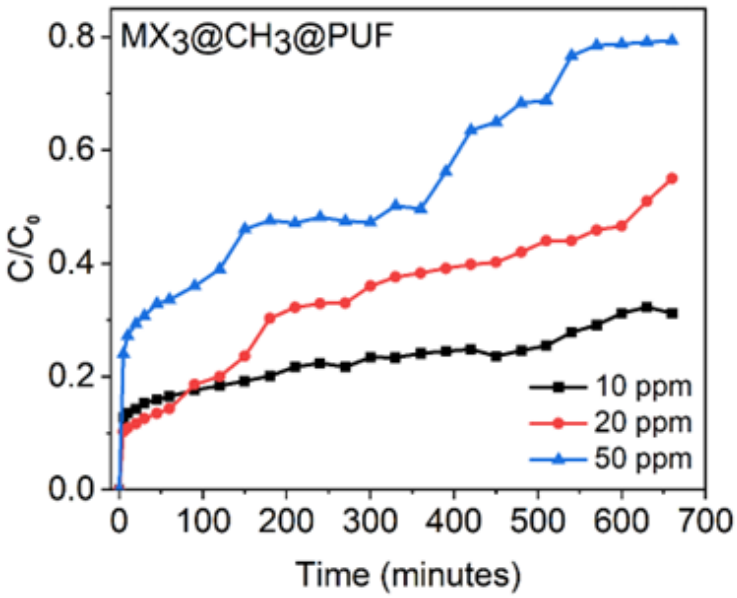

Figure 24:Breakthrough curve for MX3@CH3@PU with different initial ion concentration for Cr(VI) removal

Breakthrough curves of $MX_3@CH_3@PUF$ show that with the higher Cr(VI) ion concentration, the adsorbent gets saturated in less time (see Figure 24). For 20ppm adsorbent reached the 50% removal in 47 minutes of operation, for 20 ppm chromium solution it took 115 minutes and for 10ppm solution it reached 50% removal in 380 minutes. Therefore, in a situation where Cr(VI) concentration is high, a higher concentration of adsorbent will be required for effective performance.

4.2.3.4 Regeneration Studies

Regeneration also called recyclability is an aspect of importance for practical and economic viability. Adsorbent Regeneration experiments were performed on $MX_3@CH_3@PUF$ sample by passing 0.2M NaOH for desorption of adsorbent after each adsorption cycle. 10 ppm initial concentration was used in the following cycles to compensate for the loss of effectivity during the first operation. The reduction in the removal efficiency observed is might be due to fatigue and loss of adsorbent. Figure 25 Shows exceptional regeneration performance of $MX_3@CH_3@PUF$ for 3 adsorption-desorption cycles at 10 ppm Cr (VI) concentration.

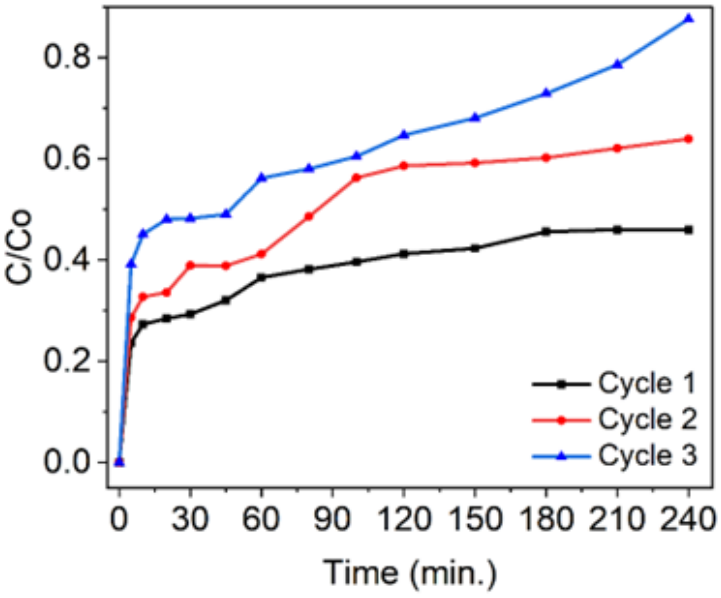

Figure 25: Breakthrough curve for regenration performance of MX3@CH3@PU

4.3 Mechanism of Cr(VI) Adsorption

Adsorption experiments were performed to understand the mechanism involved for the removal of Chromium (VI). The maximum removal percentage achieved in this study was at pH range 1.5-2.5 and 2.5 was selected as the optimum pH. In acidic conditions, the functional groups present on the surface of the adsorbent such as hydroxyl group (-OH),

carboxyl group (COOH) get protonated and adsorb the negatively charged chromium species. Moreover, at pH < 3 the dominant form of chromium is $HCrO^{4-}$ and requires only singular site for adsorption whereas, at pH > 3 the dominant forms of chromium are $Cr_2O_7^{2-}$, CrO_4^{2-} which require at least two exchangeable sites for adsorption. This electrostatic phenomenon was well supported by the kinetic and isotherm studies where the Pseudo second order (PSO) kinetic model and Freundlich Isotherm model better fit the experimental data revealing that the adsorption process is controlled through chemisorption. SEM of the adsorbent $MX_3@CH_3@PU$ after uptake of Chromium (VI) had a blocky structure which might be due to the uptake of Chromium (VI). This is also confirmed by EDS results. Moreover, the FTIR curves of $MX_3@CH_3@PU$ after uptake of Cr (VI) indicate a shift of the curve after binding of Chromium. This could be due to the complexation (Eqs.(12) - (13)) between adsorbent active sites and Cr. Ion exchange (Eq.14) process was also involved in the adsorption process. Thus, overall mechanism of Cr (VI) adsorption onto $MX_3@CH_3@PU$ involve chemical adsorption i.e., Ion exchange, electrostatic attraction, and complexation between functional groups on the surface of adsorbent and chromium.

$$R - COO^- + Cr^{6+} \; R - COO{-}Cr^{6+} \quad (12)$$

$$R - O^- + Cr^{6+} \; R - O{-}Cr^{6+} \quad (13)$$

$$R - COOH + Cr^{6+} \; R - COO{-}Cr^{6+} + H^+ \quad (14)$$

4.4 Disposal of Adsorbent

Disposal of adsorbents is also a considerable aspect of utilizing the best available materials for wastewater treatment. In this study, adsorbent disposal was kept into account and choose the best way possible to dispose of the adsorbent at the end of its life. Lin et al. has studied the fire hazards of the PU foam and showed the significant results of fire and smoke suppression effect by using chitosan and MXene layer-by-layer surface coating. The study showed 71% less smoke release 70% reduction in the formation of carbon monoxide and carbon dioxide gases and 65.5% reduction in total heat release by layer-by-layer surface coating of PU foam. This aspect makes the PU foam coated with chitosan and MXene an ideal candidate from the perspective of wastewater treatment and post-treatment handling (Lin et al., 2020).

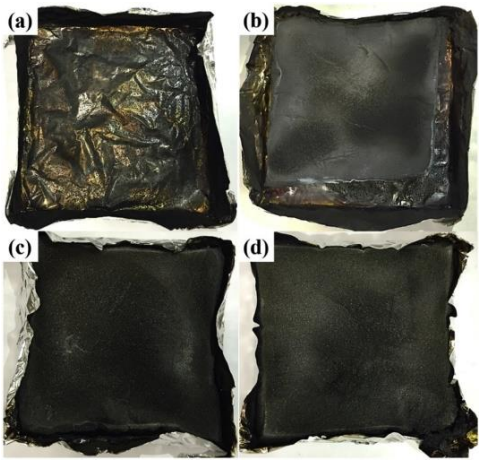

Figure 26: Disposal of PU foam adsorbent

CHAPTER 5

CONCLUSION

In this study, different adsorbents utilizing polyurethane foam (PUF) as low-cost support material have been observed for the removal of hexavalent chromium Cr (VI). The results showed that MX_3@CH_3@PUF prepared by 3 layer by layer coating was effective for chromium removal from wastewater due to high surface area and more active sites. MX_3@CH_3@PUF achieved maximum removal efficiency than other peer adsorbents. When the pH value is between 1.5 to 2.5, the removal efficiency of Cr(VI) by MX_3@CH_3@PUF reached >95% which is higher than other prepared PUF-supported adsorbents. The adsorbent data fitted better with the pseudo second order (PSO) and Freundlich isotherm model. Further investigation into Cr(VI) removal exhibits that the electrostatic attraction, ion exchange, complexation of chromium with MX_3@CH_3@PUF and reduction Cr(VI) to Cr(III) due to MXene coating are the dominating mechanism of Cr(VI) binding on the surface of MX_3@CH_3@PUF. Fixed bed adsorption studies showed the structure stability of MX_3@CH_3@PUF in continuous operations and proved to be a promising adsorbent for chromium metal removal from wastewater. Regeneration of the MX_3@CH_3@PUF showed the stability of chitosan and MXene as adsorbent materials. Overall, the adsorption cost is much lower by using PUF as support material and chitosan as a surface binder than utilizing the MXene powder for heavy metal removal.

REFERENCES

Agrafioti, E., Kalderis, D., & Diamadopoulos, E. (2014). Arsenic and chromium removal from water using biochars derived from rice husk, organic solid wastes and sewage sludge. *Journal of Environmental Management*, *133*, 309–314. https://doi.org/10.1016/J.JENVMAN.2013.12.007

Alagawany, M., Elnesr, S. S., Farag, M. R., Tiwari, R., Yatoo, M. I., Karthik, K., Michalak, I., & Dhama, K. (2021). Nutritional significance of amino acids, vitamins and minerals as nutraceuticals in poultry production and health – a comprehensive review. *The Veterinary Quarterly*, *41*(1), 1. https://doi.org/10.1080/01652176.2020.1857887

Anju, M., & Renuka, N. K. (2020). Magnetically actuated graphene coated polyurethane foam as potential sorbent for oils and organics. *Arabian Journal of Chemistry*, *13*(1), 1752–1762. https://doi.org/10.1016/J.ARABJC.2018.01.012

Aregahegn, M. (2021). *Determination and Removal of Hexavalent Chromium*.

Bohdziewicz, J. (2000). Removal of chromium ions (VI) from underground water in the hybrid complexation-ultrafiltration process. *Desalination*, *129*(3), 227–235. https://doi.org/10.1016/S0011-9164(00)00063-1

Briffa, J., Sinagra, E., & Blundell, R. (2020). Heavy metal pollution in the environment and their toxicological effects on humans. *Heliyon*, *6*(9), e04691. https://doi.org/10.1016/J.HELIYON.2020.E04691

Chen, F., Ma, J., Akhtar, S., Khan, Z. I., Ahmad, K., Ashfaq, A., Nawaz, H., & Nadeem, M. (2022). Assessment of chromium toxicity and potential health implications of agriculturally diversely irrigated food crops in the semi-arid regions of South Asia. *Agricultural Water Management*, *272*, 107833. https://doi.org/10.1016/J.AGWAT.2022.107833

Crini, G., & Badot, P. M. (2008). Application of chitosan, a natural aminopolysaccharide, for dye removal from aqueous solutions by adsorption processes using batch studies: A review of recent literature. *Progress in Polymer Science*, *33*(4), 399–447. https://doi.org/10.1016/J.PROGPOLYMSCI.2007.11.001

Danish, M. I., Qazi, I. A., Zeb, A., Habib, A., Awan, M. A., & Khan, Z. (2013). Arsenic removal from aqueous solution using pure and metal-doped titania nanoparticles coated on glass beads. *Journal of Nanomaterials*, *2013*, 17. https://doi.org/10.1155/2013/873694

Doke, S. M., & Yadav, G. D. (2014). Process efficacy and novelty of titania membrane prepared by polymeric sol-gel method in removal of chromium(VI) by surfactant enhanced microfiltration. *Chemical Engineering Journal*, *255*, 483–491. https://doi.org/10.1016/j.cej.2014.05.098

Dong, Y., Sang, D., He, C., Sheng, X., & Lei, L. (2019a). Mxene/alginate composites for lead and copper ion removal from aqueous solutions. *RSC Advances*, *9*(50), 29015–29022. https://doi.org/10.1039/C9RA05251H

Dong, Y., Sang, D., He, C., Sheng, X., & Lei, L. (2019b). Mxene/alginate composites for lead and copper ion removal from aqueous solutions. *RSC Advances*, *9*(50), 29015–29022. https://doi.org/10.1039/C9RA05251H

Elfeky, S. A., Mahmoud, S. E., & Youssef, A. F. (2017). Applications of CTAB modified magnetic nanoparticles for removal of chromium (VI) from contaminated water. *Journal of Advanced Research*, *8*(4), 435–443. https://doi.org/10.1016/J.JARE.2017.06.002

Fard, A. K., Mckay, G., Chamoun, R., Rhadfi, T., Preud'Homme, H., & Atieh, M. A. (2017). Barium removal from synthetic natural and produced water using MXene as two dimensional (2-D) nanosheet adsorbent. *Chemical Engineering Journal*, *317*, 331–342. https://doi.org/10.1016/J.CEJ.2017.02.090

Fard, A. K., Rhadfi, T., Mckay, G., Manawi, Y., Kochkodan, V., Lee, O.-S., Atieh, M. A., & Lee, -S. (2021). *Two-dimensional MXene for efficient arsenic removal from aqueous solutions: experimental and molecular dynamics simulation*. 280–295. https://doi.org/10.5004/dwt.2021.26607

Feng, Y., Wang, H., Xu, J., Du, X., Cheng, X., Du, Z., & Wang, H. (2021). Fabrication of MXene/PEI functionalized sodium alginate aerogel and its excellent adsorption behavior for Cr(VI) and Congo Red from aqueous solution. *Journal of Hazardous Materials*, *416*, 125777. https://doi.org/10.1016/J.JHAZMAT.2021.125777

Gaikwad, M. S., & Balomajumder, C. (2017). Simultaneous rejection of chromium(VI) and fluoride [Cr(VI) and F] by nanofiltration: Membranes characterizations and estimations of membrane transport parameters by CFSK model. *Journal of Environmental Chemical Engineering*, *5*(1), 45–53. https://doi.org/10.1016/j.jece.2016.11.018

Gan, D., Huang, Q., Dou, J., Huang, H., Chen, J., Liu, M., Wen, Y., Yang, Z., Zhang, X., & Wei, Y. (2020). Bioinspired functionalization of MXenes (Ti3C2TX) with amino acids for efficient removal of heavy metal ions. *Applied Surface Science*, *504*, 144603. https://doi.org/10.1016/J.APSUSC.2019.144603

Gao, Y., Yang, J., Song, X., -, al, Li, N., Guo, C., Shi, H., Chadha, U., Kumaran Selvaraj, S., Vishak Thanu, S., Cholapadath, V., Mathew Abraham, A., Zaiyan, M. M., Manoharan, M., & Paramsivam, V. (2022). A review of the function of using carbon nanomaterials in membrane filtration for contaminant removal from wastewater. *Materials Research Express*, *9*(1), 012003. https://doi.org/10.1088/2053-1591/AC48B8

Golder, A. K., Chanda, A. K., Samanta, A. N., & Ray, S. (2007). Removal of Cr(VI) from Aqueous Solution: Electrocoagulation vs Chemical Coagulation. *Http://Dx.Doi.Org/10.1080/01496390701446464*, *42*(10), 2177–2193. https://doi.org/10.1080/01496390701446464

Gonzalez-Julian, J. (2021). Processing of MAX phases: From synthesis to applications. *Journal of the American Ceramic Society*, *104*(2), 659–690. https://doi.org/10.1111/jace.17544

Gorzin, F., & Bahri Rasht Abadi, M. M. (2018). Adsorption of Cr(VI) from aqueous solution by adsorbent prepared from paper mill sludge: Kinetics and thermodynamics studies. *Adsorption Science and Technology*, *36*(1–2), 149–169. https://doi.org/10.1177/0263617416686976

Gupta, S., & Babu, B. V. (2009). Utilization of waste product (tamarind seeds) for the removal of Cr(VI) from aqueous solutions: Equilibrium, kinetics, and regeneration studies. *Journal of Environmental Management*, *90*(10), 3013–3022. https://doi.org/10.1016/J.JENVMAN.2009.04.006

Hadi, M. A., Christopoulos, S. R. G., Naqib, S. H., Chroneos, A., Fitzpatrick, M. E.,

& Islam, A. K. M. A. (2018). Physical properties and defect processes of M3SnC2 (M = Ti, Zr, Hf) MAX phases: Effect of M-elements. *Journal of Alloys and Compounds*, *748*, 804–813. https://doi.org/10.1016/J.JALLCOM.2018.03.182

Hansen, E., Perret, D., Bardez-Giboire, I., Mure, S., Panteix, P. J., Rapin, C., Hansen, E., Perret, D., Bardez-Giboire, I., Mure, S., Panteix, P. J., & Rapin, C. (2022). Chromium enriched peraluminous glasses: Incorporation limit, crystalline phase equilibrium and impact of chromium on the rheological properties of the glass. *JNuM*, *567*, 153802. https://doi.org/10.1016/J.JNUCMAT.2022.153802

Hong, H. J., Lim, J. S., Hwang, J. Y., Kim, M., Jeong, H. S., & Park, M. S. (2018). Carboxymethlyated cellulose nanofibrils(CMCNFs) embedded in polyurethane foam as a modular adsorbent of heavy metal ions. *Carbohydrate Polymers*, *195*, 136–142. https://doi.org/10.1016/J.CARBPOL.2018.04.081

Ibrahim, Y., Kassab, A., Eid, K., Abdullah, A. M., Ozoemena, K. I., & Elzatahry, A. (2020). Unveiling Fabrication and Environmental Remediation of MXene-Based Nanoarchitectures in Toxic Metals Removal from Wastewater: Strategy and Mechanism. *Nanomaterials 2020, Vol. 10, Page 885*, *10*(5), 885. https://doi.org/10.3390/NANO10050885

Ihsanullah, I. (2020). MXenes (two-dimensional metal carbides) as emerging nanomaterials for water purification: Progress, challenges and prospects. *Chemical Engineering Journal*, *388*, 124340. https://doi.org/10.1016/J.CEJ.2020.124340

Innovative water solutions for sustainable development SUMMARY. (2014).

Jun, B. M., Her, N., Park, C. M., & Yoon, Y. (2019). Effective removal of Pb(ii) from synthetic wastewater using Ti 3 C 2 T x MXene. *Environmental Science: Water Research & Technology*, *6*(1), 173–180. https://doi.org/10.1039/C9EW00625G

Kahlon, S. K., Sharma, G., Julka, J. M., Kumar, A., Sharma, S., & Stadler, F. J. (2018). Impact of heavy metals and nanoparticles on aquatic biota. *Environmental Chemistry Letters 2018 16:3*, *16*(3), 919–946. https://doi.org/10.1007/S10311-018-0737-4

Karimi-Maleh, H., Ayati, A., Ghanbari, S., Orooji, Y., Tanhaei, B., Karimi, F.,

Alizadeh, M., Rouhi, J., Fu, L., & Sillanpää, M. (2021). Recent advances in removal techniques of Cr(VI) toxic ion from aqueous solution: A comprehensive review. *Journal of Molecular Liquids*, *329*. https://doi.org/10.1016/j.molliq.2020.115062

Kumar Basumatary, A., Adhikari, P. P., Ghoshal, A. K., & Pugazhenthi, G. (2016). Fabrication and performance evaluation of Faujasite zeolite composite ultrafiltration membrane by separation of trivalent ions from aqueous solution. *Wiley Online Library*, *35*(4), 1047–1054. https://doi.org/10.1002/ep.12325

Kumari, S., Chauhan, G. S., Monga, S., Kaushik, A., & Ahn, J. H. (2016). New lignin-based polyurethane foam for wastewater treatment. *RSC Advances*, *6*(81), 77768–77776. https://doi.org/10.1039/C6RA13308H

Laureano-Anzaldo, C. M., González-López, M. E., Pérez-Fonseca, A. A., Cruz-Barba, L. E., & Robledo-Ortíz, J. R. (2021). Synthesis of silanized chitosan anchored onto porous composite and its performance in fixed-bed adsorption of Cr(VI). *Journal of Environmental Chemical Engineering*, *9*(6), 106353. https://doi.org/10.1016/J.JECE.2021.106353

Liang, M., Ding, Y., Zhang, Q., Wang, D., Li, H., & Lu, L. (2020). Removal of aqueous Cr(VI) by magnetic biochar derived from bagasse. *Scientific Reports 2020 10:1*, *10*(1), 1–13. https://doi.org/10.1038/s41598-020-78142-3

Lin, B., Yuen, A. C. Y., Li, A., Zhang, Y., Chen, T. B. Y., Yu, B., Lee, E. W. M., Peng, S., Yang, W., Lu, H. D., Chan, Q. N., Yeoh, G. H., & Wang, C. H. (2020). MXene/chitosan nanocoating for flexible polyurethane foam towards remarkable fire hazards reductions. *Journal of Hazardous Materials*, *381*, 120952. https://doi.org/10.1016/J.JHAZMAT.2019.120952

Machado Centenaro, G. S. N., Facin, B. R., Valério, A., de Souza, A. A. U., da Silva, A., de Oliveira, J. V., & de Oliveira, D. (2017). Application of polyurethane foam chitosan-coated as a low-cost adsorbent in the effluent treatment. *Journal of Water Process Engineering*, *20*, 201–206. https://doi.org/10.1016/J.JWPE.2017.11.008

Mathis, T. S., Maleski, K., Goad, A., Sarycheva, A., Anayee, M., Foucher, A. C., Hantanasirisakul, K., Shuck, C. E., Stach, E. A., & Gogotsi, Y. (2021). Modified

MAX Phase Synthesis for Environmentally Stable and Highly Conductive Ti3C2MXene. *ACS Nano*, *15*(4), 6420–6429. https://doi.org/10.1021/acsnano.0c08357

Mohamed, A., … W. E.-H.-E. and, & 2020, undefined. (n.d.). Effect of hexavalent chromium exposure on the liver and kidney tissues related to the expression of CYP450 and GST genes of Oreochromis niloticus fish. *Elsevier*. Retrieved September 6, 2022, from https://www.sciencedirect.com/science/article/pii/S0147651319312217?casa_token=Od1YZGVCG8MAAAAA:yQ6olCochXlDu1OZiuM9WlDLSf9qiNFyvio78FttV4pDMdOLyq6_35bC7FHsv9afIMUEXWw

Monga, A., Fulke, A. B., & Dasgupta, D. (2022). Recent developments in essentiality of trivalent chromium and toxicity of hexavalent chromium: Implications on human health and remediation strategies. *Journal of Hazardous Materials Advances*, *7*, 100113. https://doi.org/10.1016/J.HAZADV.2022.100113

Nidheesh, P. V. (2022). Removal of nutrients and other emerging inorganic contaminants from water by electrocoagulation process. *Elsevier*. https://www.sciencedirect.com/science/article/pii/S0045653522022494?casa_token=rv1j-P6jKi8AAAAA:tdF1dHOURwpspOotWbw24ZS7N82UkJpke5PA8WfSQJwl3x7PapJ9T9tNypvmi2fjZhY5chk

Niu, C., Zhang, N., Hu, C., Zhang, C., Zhang, H., & Xing, Y. (2021). Preparation of a novel citric acid-crosslinked Zn-MOF/chitosan composite and application in adsorption of chromium(VI) and methyl orange from aqueous solution. *Carbohydrate Polymers*, *258*, 117644. https://doi.org/10.1016/J.CARBPOL.2021.117644

Patel, H. (2019). Fixed-bed column adsorption study: a comprehensive review. *Applied Water Science 2019 9:3*, *9*(3), 1–17. https://doi.org/10.1007/S13201-019-0927-7

Peng, H., & Guo, J. (2020a). Removal of chromium from wastewater by membrane filtration, chemical precipitation, ion exchange, adsorption electrocoagulation, electrochemical reduction, electrodialysis, electrodeionization, photocatalysis and nanotechnology: a review. *Environmental Chemistry Letters 2020 18:6*,

18(6), 2055–2068. https://doi.org/10.1007/S10311-020-01058-X

Peng, H., & Guo, J. (2020b). Removal of chromium from wastewater by membrane filtration, chemical precipitation, ion exchange, adsorption electrocoagulation, electrochemical reduction, electrodialysis, electrodeionization, photocatalysis and nanotechnology: a review. *Environmental Chemistry Letters*, *18*(6), 2055–2068. https://doi.org/10.1007/S10311-020-01058-X

Peng, M., Zhu, Y., Li, H., He, K., Zeng, G., Chen, A., Huang, Z., Huang, T., Yuan, L., & Chen, G. (2019). Synthesis and application of modified commercial sponges for oil-water separation. *Chemical Engineering Journal*, *373*, 213–226. https://doi.org/10.1016/J.CEJ.2019.05.013

Ramakrishnaiah, C. R., & Prathima, B. (2012). Hexavalent Chromium Removal From Industrial Watsewater By Chemical Precipitation Method. *International Journal of Engineering Research and Applications*, *2*(2), 599–603. www.ijera.com

Reale, M. (2021). Annual Report 2021. *AIMS Allergy and Immunology*, *6*(1), 1–5. https://doi.org/10.3934/ALLERGY.2022001

Rinaudo, M. (2006). Chitin and chitosan: Properties and applications. *Progress in Polymer Science*, *31*(7), 603–632. https://doi.org/10.1016/J.PROGPOLYMSCI.2006.06.001

Rodrigues, E., Almeida, O., Brasil, H., Moraes, D., & dos Reis, M. A. L. (2019). Adsorption of chromium (VI) on hydrotalcite-hydroxyapatite material doped with carbon nanotubes: Equilibrium, kinetic and thermodynamic study. *Applied Clay Science*, *172*, 57–64. https://doi.org/10.1016/J.CLAY.2019.02.018

Santos, O. S. H., Coelho da Silva, M., Silva, V. R., Mussel, W. N., & Yoshida, M. I. (2017). Polyurethane foam impregnated with lignin as a filler for the removal of crude oil from contaminated water. *Journal of Hazardous Materials*, *324*, 406–413. https://doi.org/10.1016/J.JHAZMAT.2016.11.004

Shafiq, Q., Husnain, S. M., Shahzad, F., Taqi Mehran, M., Raza Kazmi, S. A., Mujtaba-ul-Hassan, S., Ahmad, J., & Iqbal, Z. (2021). Rational design of MXene coated polyurethane foam for the removal of Pb2+. *Materials Letters*, *304*, 130600. https://doi.org/10.1016/j.matlet.2021.130600

Shahzad, A., Nawaz, M., Moztahida, M., Jang, J., Tahir, K., Kim, J., Lim, Y., Vassiliadis, V. S., Woo, S. H., & Lee, D. S. (2019). Ti3C2Tx MXene core-shell spheres for ultrahigh removal of mercuric ions. *Chemical Engineering Journal*, *368*, 400–408. https://doi.org/10.1016/J.CEJ.2019.02.160

Shahzad, A., Rasool, K., Miran, W., Nawaz, M., Jang, J., Mahmoud, K. A., & Lee, D. S. (2017). Two-Dimensional Ti3C2Tx MXene Nanosheets for Efficient Copper Removal from Water. *ACS Sustainable Chemistry and Engineering*, *5*(12), 11481–11488. https://doi.org/10.1021/ACSSUSCHEMENG.7B02695/SUPPL_FILE/SC7B02695_SI_001.PDF

Shahzad, A., Rasool, K., Miran, W., Nawaz, M., Jang, J., Mahmoud, K. A., & Lee, D. S. (2018). Mercuric ion capturing by recoverable titanium carbide magnetic nanocomposite. *Journal of Hazardous Materials*, *344*, 811–818. https://doi.org/10.1016/j.jhazmat.2017.11.026

Siqueira, G., Bras, J., & Dufresne, A. (2010). Cellulosic bionanocomposites: A review of preparation, properties and applications. *Polymers*, *2*(4), 728–765. https://doi.org/10.3390/POLYM2040728

Sokol, M., Natu, V., Kota, S., & Barsoum, M. W. (2019). On the Chemical Diversity of the MAX Phases. *Trends in Chemistry*, *1*(2), 210–223. https://doi.org/10.1016/J.TRECHM.2019.02.016

Somen, J., Purkait, M., Science, M. K.-A. C., & 2010, undefined. (2010). Preparation and characterization of low-cost ceramic microfiltration membranes for the removal of chromate from aqueous solutions. *Cabdirect.Org*. https://www.cabdirect.org/cabdirect/abstract/20103084549

Srivastava, D., Tiwari, M., Dutta, P., Singh, P., Chawda, K., Kumari, M., Chakrabarty, D., & Sivanesan, I. (2021). Chromium stress in plants: toxicity, tolerance and phytoremediation. *Mdpi.Com*. https://doi.org/10.3390/su13094629

Velusamy, S., Roy, A., Sundaram, S., & Kumar Mallick, T. (2021). A Review on Heavy Metal Ions and Containing Dyes Removal Through Graphene Oxide-Based Adsorption Strategies for Textile Wastewater Treatment. *The Chemical Record*, *21*(7), 1570–1610. https://doi.org/10.1002/TCR.202000153

Wang, H., Cui, H., Song, X., Xu, R., Wei, N., Tian, J., & Niu, H. (2020). Facile synthesis of heterojunction of MXenes/TiO2 nanoparticles towards enhanced hexavalent chromium removal. *Journal of Colloid and Interface Science*, *561*, 46–57. https://doi.org/10.1016/J.JCIS.2019.11.120

Wang, X. S., Tang, Y. P., & Tao, S. R. (2009). Kinetics, equilibrium and thermodynamic study on removal of Cr (VI) from aqueous solutions using low-cost adsorbent Alligator weed. *Chemical Engineering Journal*, *148*(2–3), 217–225. https://doi.org/10.1016/J.CEJ.2008.08.020

Wei, X. Z., Gan, Z. Q., Shen, Y. J., Qiu, Z. L., Fang, L. F., & Zhu, B. K. (2019). Negatively-charged nanofiltration membrane and its hexavalent chromium removal performance. *Journal of Colloid and Interface Science*, *553*, 475–483. https://doi.org/10.1016/J.JCIS.2019.06.051

WHO. (2017). *Guidelines for drinking-water quality, 4th edition, incorporating the 1st addendum*. http://www.who.int/water_sanitation_health/publications/drinking-water-quality-guidelines-4-including-1st-addendum/en/

Wise, J. P., Young, J. L., Cai, J., & Cai, L. (2022). Current understanding of hexavalent chromium [Cr(VI)] neurotoxicity and new perspectives. *Environment International*, *158*, 106877. https://doi.org/10.1016/J.ENVINT.2021.106877

Xu, J., Zeng, G., Lin, Q., Gu, Y., Wang, X., Feng, Z., & Sengupta, A. (2022). Application of 3D magnetic nanocomposites: MXene-supported Fe3O4@CS nanospheres for highly efficient adsorption and separation of dyes. *Science of The Total Environment*, *822*, 153544. https://doi.org/10.1016/J.SCITOTENV.2022.153544

Yang, G., Hu, X., Liang, J., Huang, Q., Dou, J., Tian, J., Deng, F., Liu, M., Zhang, X., & Wei, Y. (2021). Surface functionalization of MXene with chitosan through in-situ formation of polyimidazoles and its adsorption properties. *Journal of Hazardous Materials*, *419*. https://doi.org/10.1016/J.JHAZMAT.2021.126220

Yaqub, A., Shafiq, Q., Khan, A. R., Husnain, S. M., & Shahzad, F. (2021). Recent advances in the adsorptive remediation of wastewater using two-dimensional transition metal carbides (MXenes): A review. *New Journal of Chemistry*, *45*(22), 9721–9742. https://doi.org/10.1039/D1NJ00772F

Yin, J., Xiong, Y., Zhou, X., Yang, Z., & Yuan, T. (2022). An efficient halogen-free reactive flame-retardant active diluent for soy-castor oil-based fire safety UV-curable coatings. *Progress in Organic Coatings*, *163*, 106683. https://doi.org/10.1016/J.PORGCOAT.2021.106683

Yu, S., Tang, H., Zhang, D., Wang, S., Qiu, M., Song, G., Fu, D., Hu, B., & Wang, X. (2022). MXenes as emerging nanomaterials in water purification and environmental remediation. *Science of The Total Environment*, *811*, 152280. https://doi.org/10.1016/J.SCITOTENV.2021.152280

Zeng, X., Wang, Y., He, X., Liu, C., Wang, X., & Wang, X. (2021). Enhanced removal of Cr(VI) by reductive sorption with surface-modified Ti3C2Tx MXene nanocomposites. *Journal of Environmental Chemical Engineering*, *9*(5), 106203. https://doi.org/10.1016/J.JECE.2021.106203

Zhang, Yanhong, Xu, X., Yue, C., Song, L., Lv, Y., Liu, F., & Li, A. (2021). Insight into the efficient co-removal of Cr(VI) and Cr(III) by positively charged UiO-66-NH2 decorated ultrafiltration membrane. *Chemical Engineering Journal*, *404*. https://doi.org/10.1016/j.cej.2020.126546

Zhang, Yujuan, Wang, L., Zhang, N., & Zhou, Z. (2018). Adsorptive environmental applications of MXene nanomaterials: a review. *RSC Advances*, *8*(36), 19895–19905. https://doi.org/10.1039/C8RA03077D

Zhu, H., Liao, Q., Wang, F., Dai, Y., & Lu, M. (2016). The effects of chromium oxide on the structure and properties of iron borophosphate glasses. *Journal of Non-Crystalline Solids*, *437*, 48–52. https://doi.org/10.1016/J.JNONCRYSOL.2016.01.013